

EFFECTS OF FEAR ON TRANSMISSION DYNAMICS OF INFECTIOUS DISEASES

EFFECTS OF FEAR ON TRANSMISSION DYNAMICS OF
INFECTIOUS DISEASES

BY
IRENA PAPST
B.Arts Sc. (Honours Mathematics)

A THESIS
SUBMITTED TO THE DEPARTMENT OF MATHEMATICS & STATISTICS
AND THE SCHOOL OF GRADUATE STUDIES
OF MCMASTER UNIVERSITY
IN PARTIAL FULFILMENT OF THE REQUIREMENTS FOR THE DEGREE OF
MASTER OF SCIENCE

© Copyright by Irena Papst, September 2015

Released under a Creative Commons Attribution-NonCommercial-ShareAlike 3.0 License
(<http://creativecommons.org/licenses/by-nc-sa/3.0/>).
Free distribution is strongly encouraged; commercial distribution is expressly forbidden.

Master of Science (2015)
(Mathematics & Statistics)

McMaster University
Hamilton, Ontario, Canada

TITLE: Effects of fear on transmission dynamics of infectious diseases

AUTHOR: Irena Papst
B.Arts Sc. (Honours Mathematics)
McMaster University, Hamilton, Ontario, Canada

SUPERVISOR: Dr. David J.D. Earn

NUMBER OF PAGES: [x, 93](#)

Abstract

An epidemiological model that incorporates individual adoption of protective behaviours due to fear of contracting an infectious disease is presented. These adaptive behaviours are assumed to lower an individual's risk of infection. The dynamics of this model are analyzed and the effects of fear on important public health metrics such as outbreak length, final size, and peak prevalence are investigated. It is concluded that the coupled dynamics of fear- and disease-spread are rich and can lead to counter-intuitive effects on the public health metrics considered. In particular, it is not always the case that more effective protective behaviours lead to the most favourable population-level outcomes; intermediate levels of effectiveness are optimal in some cases. This result depends on when fearful individuals become infected with respect to the main outbreak that is mostly driven by the infection of fully susceptible individuals.

Acknowledgments

First and foremost, I am forever indebted to my supervisor, Dr. David Earn. He has been my academic mentor and friend for a little over the last three years, and I cannot thank him enough for all that he has done for me. David, thank you, above all, for believing in me even when I didn't believe in myself. There is always a quad shot latte waiting for you in Ithaca.

Thank you to Drs. Ben Bolker and Jonathan Dushoff for being part of my examining committee, for providing thoughtful suggestions and comments on the draft of this work, and for inviting me to speak in their scientific session at the 2014 CMS Winter Meeting. Special thanks to Dr. Bolker for our discussions after my winter meeting talk as they helped shape the better part of chapter 3.

I would also like to thank both past and present members of Earnlab (David Champredon, Sarah Drohan, Karsten Hempel, Michelle deJonge, Susan Marsh-Rollo, Chai Molina, and Dora Rosati) for being supportive and enthusiastic colleagues these last three years, and to David for working so hard to create a community among his students. I will *never* forget that time we **beat Pandemic**. I would say more, but I have to get back to juggling practice.

Thanks to all members of the math Phoenix trivia team for persistently working hard to take down our archnemesis, Biocurious, week after week.

A special thank you to my good friend, roommate, and fellow math bio disciple, Spencer Hunt. It has been an absolute pleasure navigating grad school life together and although our paths have diverged, I know that you will eventually return to where you belong (within 10 minutes of a Metro burrito at all times).

This thesis would not have been possible without the support of all of my friends outside of the math department. Sheridan, thank you for keeping me sane and unbelievably happy these past few months (but mostly for introducing me to the magic of baseball). Natalie and Dimitri, you have been my best friends for 11 years

now (nearly half of my life!), and I look forward to making many more memories with you (which Natalie will inevitably have to remind me of because of my poor memory). Sam, it's an honour to call myself your good friend and co-chef in pizza.

Lastly, and most importantly, thank you to my parents, Predrag and Ljiljana, my grandparents, Mirko and Danica, and my aunt, Gordana, for being my biggest supporters my entire life. Volim vas do neba.

Over the course of my Master's degree, I was supported by a Natural Sciences and Engineering Research Council of Canada (NSERC) Alexander Graham Bell Canada Graduate Scholarship, and an Ontario Graduate Scholarship. Moreover, my first research experience with Dr. Earn was supported by an NSERC Undergraduate Student Research Award. Without these funding initiatives, I would likely not be where I am today (that is, free of crippling debt). Thank you to the Canadian federal and Ontario provincial governments for providing me with this valuable financial support.

Contents

Abstract	iii
Acknowledgments	iv
1 Introduction	1
2 Models	3
2.1 The SIR Model	3
2.1.1 Equations	4
2.1.2 Assumptions	4
2.1.3 Analysis	5
2.2 The Behavioural SIR with Prevalence-Based Fear (bSIR-P)	8
2.2.1 Equations	9
2.2.2 Assumptions	11
2.2.3 Analysis	12
2.3 The Behavioural SIR with Prevalence- and Fear-Based Fear (bSIR-PF)	17
2.3.1 Equations	20
2.3.2 Assumptions	20
2.3.3 Analysis	21
2.4 The Effect of Fear on Prevalence Patterns	23

3 Simplifying the bSIR Models	27
3.1 Basic SIR Fitting	27
3.2 Fast-Fear Approximation	32
4 The Effects of Fear on Public Health Metrics	38
4.1 The Behavioural SIR with Prevalence-Based Fear (bSIR-P)	40
4.1.1 Outbreak Length	40
4.1.2 Final Size	45
4.1.3 Peak Prevalences	47
4.2 The Behavioural SIR with Prevalence- and Fear-Based Fear (bSIR-PF)	49
4.2.1 Outbreak Length	49
4.2.2 Final Size	54
4.2.3 Peak Prevalences	56
4.3 Discussion	58
5 Conclusion	59
A Proof of Lemma 1	65
B Sample Code for SIR Fitting	69
B.1 Preliminaries	69
B.2 Numerically Solving the bSIR Equations	69
B.2.1 Compiled Gradient	70
B.2.2 Numerical Integration Script	72
B.2.3 Generating bSIR Data	73
B.3 Fitting an SIR Model to bSIR Data	76
C Sample Code for Calculating Public Health Quantities	79
C.1 Preliminaries	79

C.2	Numerically Solving the bSIR Equations	79
C.3	Number of Epidemic Peaks	79
C.4	Epidemic Length	81
C.5	Final Size	82
C.6	Peak Prevalences	83
D	Full Results from Chapter 4: The Effects of Fear on Public Health Quantities	86
D.1	The Behavioural SIR with Prevalence-Based Fear (bSIR-P)	86
D.1.1	Outbreak Length	86
D.1.2	Final Size	88
D.1.3	Peak Prevalences	89
D.2	The Behavioural SIR with Prevalence- and Fear-Based Fear (bSIR-PF)	90
D.2.1	Outbreak Length	91
D.2.2	Final Size	92
D.2.3	Peak Prevalences	93

List of Figures

2.1	SIR model flow chart	4
2.2	bSIR-P model flow chart	10
2.3	bSIR-PF model flow chart	19
2.4	SIR model: a single epidemic	23
2.5	bSIR-P model: multiple waves of infection	24
2.6	bSIR-P model: prevalence of fear during multiple waves of infection	26
3.1	Plots of SIR model fits to simulated bSIR-P prevalence data	29
3.2	Plots of fast-fear approximation fits where fear transmits more quickly than disease.	34
3.3	Fraction fearful at the fast-fear equilibrium as a function of prevalence	36
4.1	Outbreak length (time to extinction) as a function of the effectiveness of fear in the bSIR-P model	42
4.2	The proportion of susceptibles, fearful susceptibles, and infected individuals over time for values of the effectiveness of fear near the threshold between one and two waves of infection in the bSIR-P model	44
4.3	Final size as a function of the effectiveness of fear in the bSIR-P model	46
4.4	Peak prevalence of each epidemic as a function of the effectiveness of fear in the bSIR-P model	48
4.5	Outbreak length (time to extinction) as a function of the effectiveness of fear in the bSIR-PF model	52

4.6	The proportion of susceptibles, fearful susceptibles, and infected individuals over time for values of the effectiveness of fear at and around the critical value that provokes the maximal time to extinction in the bSIR-PF model	53
4.7	Final size as a function of the effectiveness of fear in the bSIR-PF model	55
4.8	Peak prevalence of each epidemic as a function of the effectiveness of fear in the bSIR-PF model	57
D.1	Supplementary plots of epidemic length (time to extinction) as a function of the effectiveness of fear in the bSIR-P model	87
D.2	Supplementary plots of final size as a function of the effectiveness of fear in the bSIR-P model	88
D.3	Supplementary plots of the peak prevalence of each epidemic as a function of the effectiveness of fear in the bSIR-P model	89
D.4	Supplementary plots of epidemic length (time to extinction) as a function of the effectiveness of fear in the bSIR-PF model	91
D.5	Supplementary plots of final size as a function of the effectiveness of fear in the bSIR-PF model	92
D.6	Supplementary plots of the peak prevalence of each epidemic as a function of the effectiveness of fear in the bSIR-PF model	93

Chapter 1

Introduction

Mathematical models have proven themselves to be a very powerful tool in the study of biological systems [1–3]. They are especially useful in fields where controlled experiments are often impossible, such as in epidemiology [4–6]. When modelling, there is a fine balance between incorporating enough detail about a system so that the model is sufficiently faithful to reality, but not so much detail that it becomes difficult to identify the mechanisms that give rise to observed patterns.

In a simple case of epidemiological modelling, one can assign a disease state to each individual in the population at any given point in time; that is, each person is either susceptible to the disease, infectious, or removed from the disease transmission process. Then, the spread of the disease is governed by the rates of disease transmission and individual recovery, which dictate the rate of change from one state to another. Within this framework, the infectious disease process can be modelled by a system of ordinary differential equations (ODEs) in time. It has been well-established that such models accurately represent the spread of infectious diseases in many cases [3–8].

However, the simplest of these models represent infectious disease spread as a rather immutable process, neglecting the dynamics that arise from active human decision-making. Over the course of an outbreak, it is unrealistic to expect individuals to conduct themselves just as they do when there is no risk of infection; instead, one might expect people to try and reduce their individual risk by any realistic means (washing their hands more often, avoiding public places and/or contact with infectious people, etc.) [9–12]. These special disease-induced behaviours are not captured in standard models. Yet, in some historical epidemics, observed patterns

(such as multiple waves of infection) can likely not be explained without accounting for self-initiated changes in individual behaviour [13–16].

As a result, there have been a number of recent studies exploring various methods of implementing adaptive human behaviour in the context of infectious disease spread [10–12, 17, 18].

One such study proposes a new class of infectious disease models wherein individuals are not only susceptible to the infection, but they can also become fearful of contracting the disease (represented by a new disease state in the model), which leads them to modify their regular behaviour in hopes of reducing their risk of infection [19]. This class of models is particularly interesting as it is not overly complicated but still yields rich dynamics to study: the coupled dynamics of infection and disease-induced fear.

In this thesis, I explore two epidemic models that incorporate behavioural changes due to fear: changes that affect the disease transmission process. In chapter 2, I precisely define these models and derive their asymptotic behaviour. I also explore the types of epidemics that these models can predict. In chapter 3, I attempt to approximate the simpler behavioural model in two ways to better understand its complex dynamics. Finally, in chapter 4, I consider the effect of including fear in a disease model on important public health metrics (specifically epidemic length, final size, and peak prevalence) and analyze the results.

Chapter 2

Models

In order to construct a model that accounts for behavioural changes due to fear, we consider a basic epidemic model—the **susceptible-infected-removed** (SIR) epidemic model—and add a fearful reaction to the disease. In this chapter, we formally introduce the SIR model, followed by two related behavioural models, and analyze all three. We only present results for the SIR model that have analogous results in the behavioural models. In the analysis, we prove the asymptotic behaviour of one of the models with fear.

2.1 The SIR Model

Individuals in a (closed) population are assigned a disease state at each point in time: **susceptible** to the infection, **infected** with the pathogen, and **removed** from the infection process (no longer infected and immune to re-infection). We use the state variables S , I , and R respectively to keep track of the proportion of the population in each disease state.

In this simple scenario, only two disease processes are modelled: infection, where infectious individuals can transmit the pathogen to susceptible individuals through contact at the *per capita disease transmission rate* βI , and recovery, where infected individuals recover at the *per capita disease recovery rate* γ .

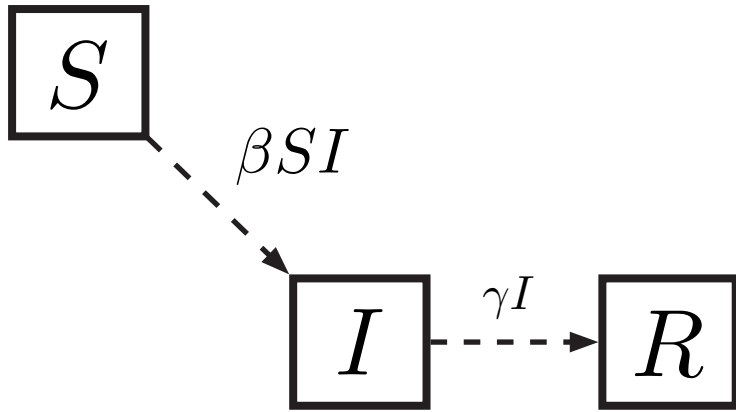


Figure 2.1: A flow chart of the simple SIR model, where S , I , and R are proportions of the population that are susceptible, infected, or removed, respectively, β is the disease transmission rate, and γ is the disease recovery rate.

2.1.1 Equations

A flow chart for this model is given in figure 2.1. We can express the model as a system of three ordinary differential equations (ODEs):

$$\frac{dS}{dt} = -\beta SI, \quad (2.1a)$$

$$\frac{dI}{dt} = \beta SI - \gamma I, \quad (2.1b)$$

$$\frac{dR}{dt} = \gamma I. \quad (2.1c)$$

2.1.2 Assumptions

As with any mathematical model, there are underlying assumptions being made in the model's construction. The SIR model assumptions are stated explicitly as follows:

- A1.** The outbreak being modelled occurs on a much faster timescale than demographic processes, including births, natural deaths, and immigration/emigration. As a result, vital dynamics can be ignored and so the population of

individuals is effectively closed.

- A2.** Once recovered, individuals are completely and permanently immune to the infection.
- A3.** Infected individuals are immediately infectious; the incubation period is negligible.
- A4.** The disease transmission is accurately described by frequency-dependent (mass action) transmission [6, 8].
- A5.** The infectious period is exponentially distributed about the mean $1/\gamma$ [20, Lecture 4].

2.1.3 Analysis

The SIR model has been analysed exhaustively (see [6, 8, 20]). Here, we only present results for the SIR model with analogous results in the models incorporating behavioural changes due to fear (discussed in sections 2.2 and 2.3).

Firstly, the SIR model is biologically well-defined, in the sense that if biologically reasonable initial conditions are given, then the solution never becomes biologically ill-defined as time goes on. More specifically, for the system of ODEs (2.1) with positive parameter values, if $0 \leq S(0) + I(0) \leq 1$ with $S(0), I(0) \geq 0$, then $0 \leq S(t) + I(t) \leq 1$ and $S(t), I(t) \geq 0$ for all times greater than zero. In other words, the domain

$$D := \{(S, I) \in \mathbb{R}^2 \mid (S \geq 0), (I \geq 0), (S + I \leq 1)\} \quad (2.2)$$

is forward invariant. The proof is omitted for brevity, but it can be found in [20, Lecture 4].

An important epidemiological quantity is the **basic reproduction number**, denoted \mathcal{R}_0 , which is the average number of secondary cases caused by a typical primary case in a wholly susceptible population [6]. This quantity gives a sense of how infectious a disease is. In the SIR model, the basic reproduction number is the rate at which new infections are produced (the transmission rate, β) multiplied by the average amount of time a person is infectious (the mean infectious period, $1/\gamma$):

$$\mathcal{R}_0 = \frac{\beta}{\gamma}. \quad (2.3)$$

The basic reproduction number must be sufficiently large for there to be an epidemic. Specifically,

$$\frac{dI}{dt} = \beta SI - \gamma I \quad (2.4a)$$

$$= (\beta S - \gamma)I \quad (2.4b)$$

$$= (\mathcal{R}_0 S - 1)\gamma I \quad (2.4c)$$

$$\leq 0 \quad \forall t \geq 0, \quad (2.4d)$$

as long as $\mathcal{R}_0 \leq 1$, since $0 \leq S(t) \leq 1$ and $I(t) \geq 0 \forall t \geq 0$ from the fact that the domain (2.2) is forward invariant, and $\gamma > 0$ by assumption. In other words, dI/dt will always be non-increasing if $\mathcal{R}_0 \leq 1$, and so no epidemic can occur. Thus, we need that $\mathcal{R}_0 > 1$ for the SIR model to predict an epidemic.

The **effective reproduction number**, \mathcal{R}_{eff} , is the average number of secondary cases a primary case will generate based on the current proportion of susceptibles in the population. For the SIR model,

$$\mathcal{R}_{\text{eff}}(t) = \mathcal{R}_0 S(t). \quad (2.5)$$

Since we assume that the population has no previous experience with the disease, no one has retained immunity from a previous outbreak, and thus $R(0) = 0$. In addition, in the limit where the population is arbitrarily large ($N \rightarrow \infty$), $I(0) \rightarrow 0$ and $S(0) \rightarrow 1$, which means that $\mathcal{R}_{\text{eff}}(0) \rightarrow \mathcal{R}_0$, a result that is consistent with the definition of both quantities. Furthermore, with the effective reproduction number defined, (2.4c) can be rewritten as

$$\frac{dI}{dt} = (\mathcal{R}_{\text{eff}} - 1)\gamma I, \quad (2.6)$$

which shows that, for the disease to spread (*i.e.*, for $I(t)$ to increase), we must have that $\mathcal{R}_{\text{eff}} > 1$. For the epidemic to peak, we must have that $\mathcal{R}_{\text{eff}} = 1$, *i.e.*, $S(t) = 1/\mathcal{R}_0$. Lastly, for the epidemic to turn over, we must have that $\mathcal{R}_{\text{eff}} < 1$.

Equilibria

The only equilibria of the SIR model are of the form

$$(S(t), I(t)) = (S_0, 0) \quad (2.7)$$

for any $0 \leq S_0 \leq 1$. These equilibria are referred to as **disease-free equilibria** since $I = 0$.

Defining the vector field associated with the system of ODEs (2.1) as

$$F(S, I) = \begin{pmatrix} -\beta SI \\ \beta SI - \gamma I \end{pmatrix}, \quad (2.8)$$

the Jacobian is computed as

$$DF_{(S,I)} = \begin{pmatrix} -\beta I & -\beta S \\ \beta I & \beta S - \gamma \end{pmatrix}. \quad (2.9)$$

Plugging in the equilibria,

$$DF_{(S_0,0)} = \begin{pmatrix} 0 & -\beta S_0 \\ 0 & \beta S_0 - \gamma \end{pmatrix}, \quad (2.10)$$

and so the eigenvalues are $\lambda_1 = 0$ and $\lambda_2 = \beta S_0 - \gamma$, meaning that the linearization always features one zero eigenvalue, regardless of the value of S at the equilibrium. Thus, all equilibria are non-hyperbolic in this system.

As a result, the linearization of the system cannot be used to determine the stability of any equilibrium point. However, one might suspect the equilibria are asymptotically stable since they occur when there is no disease and there is a finite population of susceptibles with only one way to flow through the compartments of the model: from susceptible, to infectious, and lastly to removed. Moreover, the biologically-relevant domain D , as given in (2.2), is forward invariant, and so solutions cannot escape it. Since there is no way to replenish the number of susceptibles to sustain the infection, one might suspect that all initial states in the domain will tend to a disease-free state.

Indeed, the set of disease-free equilibria of the form (2.7) are globally asymptotically stable when $\mathcal{R}_0 > 0$ [5]; all initial states will eventually converge to the disease-free state. Since it is required that $\mathcal{R}_0 > 1$ for an epidemic to occur, then the final size of an epidemic (defined as the total number of cases over the entire epidemic) is well-defined for the SIR model with $\mathcal{R}_0 > 1$.

2.2 The Behavioural SIR with Prevalence-Based Fear (bSIR-P)

To incorporate behavioural changes due to fear of infection into the basic SIR model, a new disease state called **fearful susceptible** is introduced, where the proportion of the population in this state is denoted by S_F . Fearful susceptibles adopt some sort of behavioural changes (such as social distancing and/or being more diligent about avoiding potential routes of transmission) which reduce their personal risk of becoming infected.

In the model, susceptibles can only become fearful through contact with infected individuals at a **fear transmission rate** of β_F ; fear spreads solely when susceptible individuals witness symptoms of the disease first-hand. (A model where, in addition to prevalence-based fear spread, fearful individuals can transmit their fear to susceptible individuals is explored in section 2.3.)

Fearful susceptibles can still become infected through contact with infected individuals, but at a reduced disease transmission rate of $r_\beta \beta$, where $0 \leq r_\beta \leq 1$. The parameter r_β is called the **proportion of the full disease transmission rate for fearful individuals**. The smaller this proportion, the more effective behavioural changes are at preventing disease spread.

Lastly, fearful individuals can recover from their fear by interacting with “healthy” individuals (that is, susceptibles, other fearful susceptibles, or removed individuals) at the **fear recovery rate** γ_F . The assumption that fearful individuals count as healthy individuals in the recovery from fear process is consistent with the previous assumption that fear can only spread when susceptible individuals witness symptoms of the disease. If the spread of fear requires a first-hand experience with the disease, than the recovery from fear should be based solely on an absence of witnessing disease symptoms. Thus, all individuals that are not infected count as “healthy” in this model, regardless of whether they are fearful or not.

For clarity and brevity, this model shall be referred to as the “bSIR-P” model (behavioural SIR with Prevalence-based spread of fear).

This model is very similar to Model I constructed and analysed by Perra *et al.* [19]. The only difference is that, in our model, “healthy” individuals are assumed to be all those who are not infected (that is, proportion $1 - I$ of the population), while Perra *et al.* assume that “healthy” individuals are only those who are susceptible or removed (that is, proportion $S + R$). This difference is only important to the recovery

Symbol	Meaning	Units
t	time	days
S	proportion of susceptible individuals	—
S_F	proportion of fearful susceptible individuals	—
I	proportion of infected individuals	—
R	proportion of removed individuals	—
β	disease transmission rate	1/days
γ	disease recovery rate	1/days
β_F	fear transmission rate	1/days
r_β	proportion of full disease transmission rate for fearful individuals	—
γ_F	fear recovery rate	1/days
r_{β_F}	proportion of full fear transmission for fear-based spread of fear	—

Table 2.1: A table of notation used, the meaning of each symbol, and units.

from fear process (the force of which relies on the proportion of “healthy” people), and so some of the analysis presented in [19] applies to the bSIR-P model as well, though numerical results will differ. In this thesis, I seek to analyze the behavioural model presented here in a more rigorous manner than in [19].

A summary of all bSIR-P model parameters, along with units, can be found in table 2.1.

2.2.1 Equations

A flow chart of this model is given in figure 2.2. This model can be cast as a system of four ODEs:

$$\frac{dS}{dt} = \gamma_F S_F (1 - I) - \beta S I - \beta_F S I, \quad (2.11a)$$

$$\frac{dS_F}{dt} = \beta_F S I - r_\beta \beta S_F I - \gamma_F S_F (1 - I), \quad (2.11b)$$

$$\frac{dI}{dt} = \beta S I + r_\beta \beta S_F I - \gamma I, \quad (2.11c)$$

$$\frac{dR}{dt} = \gamma I. \quad (2.11d)$$

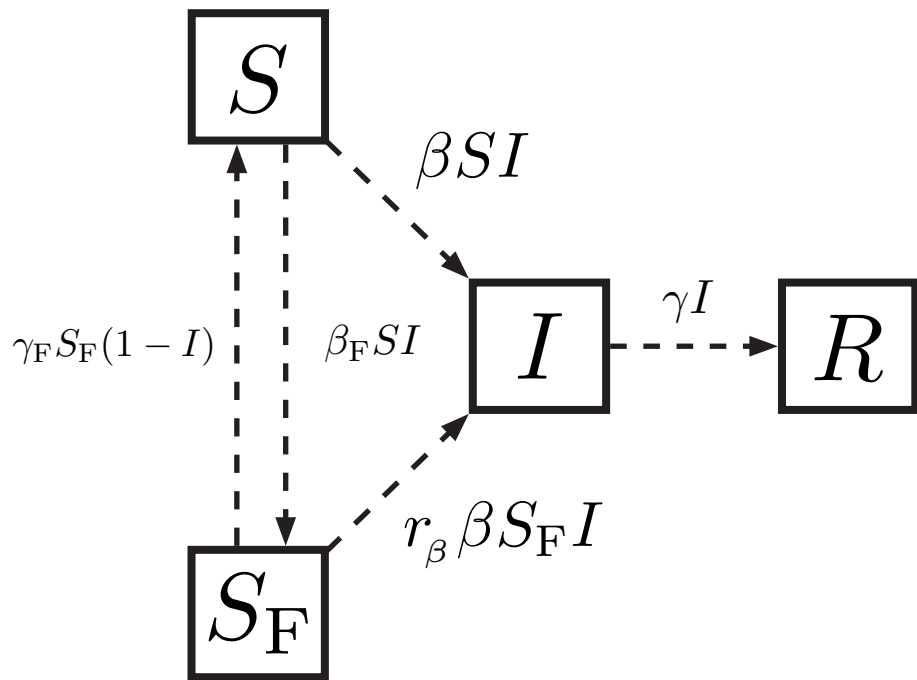


Figure 2.2: A flow chart of the bSIR-P model, where, in addition to the basic state variables and parameters from the SIR model, S_F is the proportion of the population that is fearful and susceptible, β_F is the fear transmission rate, γ_F is the fear recovery rate, and r_β is the proportion of the full disease transmission rate β applied to the infection of fearful susceptibles.

Since the first three equations do not depend on the state variable R , and the population is assumed to be closed such that

$$S(t) + S_F(t) + I(t) + R(t) = 1, \quad \forall t \geq 0, \quad (2.12)$$

then $R(t) = 1 - S(t) - S_F(t) - I(t)$ for all $t \geq 0$, which makes equation (2.11d) redundant.

2.2.2 Assumptions

The bSIR-P model shares all of the same basic assumptions as the SIR model, as well as the following additional assumptions:

- A6.** Fear spreads to susceptible individuals by contact with those infected with the disease (infecteds) through frequency-dependent transmission.
- A7.** Fearful susceptibles recover from fear by contact with “healthy” individuals (all those who are not infected), also in a frequency-dependent manner.
- A8.** The infection is non-lethal and removed individuals appear indistinguishable from susceptible or fearful individuals (removed individuals are also “healthy”).
- A9.** Fearful susceptibles can still be infected with the disease at a reduced transmission rate (provided $r_\beta \neq 0, 1$). In the case where $r_\beta = 0$, fearful individuals are perfectly (self-)quarantined. In the case where $r_\beta = 1$, all susceptible individuals (whether they are fearful or not) are subject to the same (full) disease transmission rate.

In addition, we assume that the disease under consideration is newly invading. Specifically:

- A10.** The population has no previous experience with this particular pathogen, and so there is no pre-existing immunity in the population.
- A11.** There is one initially infectious individual to seed the potential epidemic.

Under these assumptions, $I(0) = 1/N$, where N is the population size, and $R(0) = 0$. Since fear is prevalence-driven, the initial proportion of infecteds is low (in a large population), and the population is assumed to have no previous experience

with the infection, we assume that $S_F(0) = 0$. By equation (2.12), $S(0) = 1 - I(0) = 1 - 1/N$.

The initial condition

$$(S, S_F, I, R)(0) = \left(1 - \frac{1}{N}, 0, \frac{1}{N}, 0\right) \quad (2.13)$$

is assumed throughout this thesis, as is a population size of $N = 10^6$. However, the results of this study will hold more generally, provided N is large and $I(0) \ll N$.

2.2.3 Analysis

Firstly, we note that this model is biologically well-defined. In particular:

Lemma 1. *For the system of ODEs (2.11) with positive parameter values, if*

$$0 \leq S(0) + S_F(0) + I(0) + R(0) \leq 1, \quad S(0), S_F(0), I(0), R(0) \geq 0, \quad (2.14)$$

then

$$0 \leq S(t) + S_F(t) + I(t) + R(t) \leq 1, \quad S(t), S_F(t), I(t), R(t) \geq 0 \quad \forall t \geq 0. \quad (2.15)$$

Proof. See appendix A. □

For the bSIR-P model, the basic reproduction number is the same as for the SIR model: $\mathcal{R}_0 = \beta/\gamma$. To understand why this is the case, note that the basic reproduction number is calculated for one primary case in a wholly susceptible population, which is exactly the initial condition assumed for the behavioural models. When there are no fearful individuals (as is assumed initially) the model reduces to the basic SIR. Thus, the basic reproduction number is the same for both models.

Similarly, the basic reproduction number must be sufficiently large to provoke an epidemic. Note that

$$\frac{dI}{dt} = \beta SI + r_\beta \beta S_F I - \gamma I \quad (2.16a)$$

$$= (\beta S + r_\beta \beta S_F - \gamma) I \quad (2.16b)$$

$$= (\mathcal{R}_0[S + r_\beta S_F] - 1) \gamma I. \quad (2.16c)$$

As with the SIR model, for a newly-invading disease in an arbitrarily large population (*i.e.*, as $N \rightarrow \infty$), $I(0) \rightarrow 0$, and so $S(0) \rightarrow 1$. Moreover, it is assumed that $S_F(0) = 0$, and so initially, (2.16c) approaches

$$\frac{dI}{dt} = (\mathcal{R}_0 - 1)\gamma I \quad (2.17)$$

Thus, for an epidemic to occur, we must have that $\mathcal{R}_0 > 1$.

Recall that the effective reproduction number is the basic reproduction number discounted by the proportion of currently available susceptibles. However, in the bSIR-P model, not all susceptibles are subject to the same transmission rate, and so this difference must be taken into account:

$$\mathcal{R}_{\text{eff}}(t) = \frac{\beta}{\gamma}S(t) + \frac{r_\beta\beta}{\gamma}S_F(t), \quad (2.18a)$$

$$= \frac{\beta}{\gamma}[S(t) + r_\beta S_F(t)], \quad (2.18b)$$

$$= \mathcal{R}_0[S(t) + r_\beta S_F(t)], \quad (2.18c)$$

$$= \mathcal{R}_0 S_{\text{eff}}(t), \quad (2.18d)$$

where

$$S_{\text{eff}} = S(t) + r_\beta S_F(t) \quad (2.19)$$

is the **effective proportion of susceptibles**. In essence, fearful susceptibles are not “worth” as much as regular susceptibles, in terms of their capacity to become infected. Thus, \mathcal{R}_0 is adjusted by the proportion S_{eff} —the *effective* proportion of susceptibles—in the calculation of \mathcal{R}_{eff} , instead of $S_{\text{tot}}(t) = S(t) + S_F(t)$, which is simply the **total proportion of susceptibles**.

Having defined \mathcal{R}_{eff} , (2.11b) can be rewritten as

$$\frac{dI}{dt} = (\mathcal{R}_{\text{eff}} - 1)\gamma I, \quad (2.20)$$

which is identical to the SIR version given in (2.6) (except that the definition of \mathcal{R}_{eff} is different in each model). Again, the epidemic can only grow, peak, or decline if $\mathcal{R}_{\text{eff}} > 1$, $\mathcal{R}_{\text{eff}} = 1$ (and so $S_{\text{eff}} = S + r_\beta S_F = 1/\mathcal{R}_0$), and $\mathcal{R}_{\text{eff}} < 1$, respectively.

Equilibria

Similarly to the SIR model, the only equilibria of the bSIR-P model are **disease-and fear-free equilibria** of the form

$$(S(t), S_F(t), I(t)) = (S_0, 0, 0) \quad (2.21)$$

for any $0 \leq S_0 \leq 1$. It is not sufficient for $I = 0$ to halt all fear processes, as the force of recovery from fear is proportional to $1 - I$. Thus, it really must be the case that $S_F = 0$ at equilibrium.

Computing the Jacobian,

$$DF_{(S,S_F,I)} = \begin{pmatrix} -\beta I - \beta_F I & \gamma_F(1-I) & -\gamma_F S_F - \beta S - \beta_F S \\ \beta_F I & -r_\beta \beta I - \gamma_F(1-I) & \beta_F S - r_\beta \beta S_F + \gamma_F S_F \\ \beta I & r_\beta \beta I & \beta S + r_\beta \beta S_F - \gamma \end{pmatrix}, \quad (2.22)$$

and plugging in the equilibria,

$$DF_{(S_0,0,0)} = \begin{pmatrix} 0 & \gamma_F & -\beta S_0 - \beta_F S_0 \\ 0 & -\gamma_F & \beta_F S_0 \\ 0 & 0 & \beta S_0 - \gamma \end{pmatrix}, \quad (2.23)$$

we see that the eigenvalues of the Jacobian are $\lambda_1 = 0$, $\lambda_2 = -\gamma_F$, $\lambda_3 = \beta S_0 - \gamma$. Since there is always one zero eigenvalue, regardless of the values of S and S_F at equilibrium, all of the equilibria in this system are non-hyperbolic, and so one cannot linearize about these equilibria to conduct a stability analysis.

In [19], Perra *et al.* perform a linearization of their model about the disease-and fear-free equilibrium $(S, S_F, I) = (1, 0, 0)$ to conclude that, if $\mathcal{R}_0 > 1$, then fear will spread in the population. However, the linearization of their model about this equilibrium is identical to the linearization of the bSIR-P model given in (2.23) about this same equilibrium ($S_0 = 1$), and so this equilibrium is also non-hyperbolic in their model. As a result, their argument is invalid. That is not to say that the conclusion they draw does not hold; it may very well be the case that fear will spread provided $\mathcal{R}_0 > 1$, but it is not supported by the argument presented in [19].

Although the disease- and fear- free equilibria are non-hyperbolic and so we cannot rely on the linearization of the model about these points to infer their stability, we can perform an alternative analysis. Just as with the SIR model, there is a finite population of susceptibles, and the change in the *total* number of susceptibles, that

is $S_{\text{tot}}(t) = S(t) + S_F(t)$, obeys the differential equation

$$\frac{dS_{\text{tot}}}{dt} = -\beta SI - r_\beta \beta S_F I \quad (2.24a)$$

$$= -\beta(S + r_\beta S_F)I \quad (2.24b)$$

$$= -\beta S_{\text{eff}} I \quad (2.24c)$$

$$\leq 0 \quad t \geq 0. \quad (2.24d)$$

which, combined with the fact that $S_{\text{tot}}(t)$ must be continuous¹, means that $S_{\text{tot}}(t)$ is non-increasing over time. In fact, $dS_{\text{tot}}/dt < 0$ provided $S_{\text{eff}}, I > 0$, and so, in this case, S_F is strictly decreasing. If either $S_{\text{eff}} = 0$ or $I = 0$, there can be no infection, which is not the case that we want to consider. Therefore, provided there are both susceptible and infectious individuals in the population, the net susceptible flow will be toward the infectious compartment, from which individuals can only move into the removed compartment.

As a result, one might expect a similar outcome as in the SIR model: all (biologically well-defined) initial states eventually converge to a disease-free state. However, in this model, if there is no disease, then there is no way to sustain fear (since fear is prevalence-driven), and so one might also expect all initial states to converge to a fear-free state as well.

Given this intuition, we want to prove that all initial conditions $(S(0), S_F(0), I(0)) \in \Delta$, where

$$\Delta := \{(S, S_F, I) \in \mathbb{R}^3 \mid (S \geq 0), (S_F \geq 0), (I \geq 0), (0 \leq S + S_F + I \leq 1)\} \quad (2.25)$$

converge to some disease- and fear-free equilibrium of the form $(S_\infty, 0, 0)$, where $0 \leq S_\infty \leq 1$. Equivalently, we want to prove the following theorem:

Theorem 1. *For the system (2.11), the set of disease- and fear-free equilibria,*

$$\mathcal{E} = \{(S, S_F, I) \in \Delta \mid S_F = I = 0\}, \quad (2.26)$$

is a closed invariant set that is globally attracting.

Proof. We will first prove that the disease-free set

$$\mathcal{C} = \{(S, S_F, I) \in \Delta \mid I = 0\} \quad (2.27)$$

¹See proof of theorem 1.

is globally attracting, and then we will show that all initial states in \mathcal{C} are attracted to its subset \mathcal{E} .

Firstly, note that for $S_{\text{tot}}(t) = S(t) + S_F(t)$,

$$\frac{dS_{\text{tot}}}{dt} = -\beta(S + r_\beta S_F)I = -\beta(S_{\text{eff}})I \leq 0 \quad \forall t \geq 0 \quad (2.28)$$

in the forward-invariant region Δ since $S, S_F, I \geq 0$ by lemma 1. Moreover, the derivatives given in (2.11) are C^∞ , and so in particular, they are C^1 , which means that the flow of this system is continuous in time². If the flow is continuous, that means that all solution trajectories $\phi(t) = (S(t), S_F(t), I(t))$ are continuous, *i.e.*, all of its components (given by the state variables) are also continuous functions of time. Thus, a linear combination of state variables, such as $S_{\text{tot}}(t) = S(t) + S_F(t)$, is also continuous for any solution. Lastly, $S_{\text{tot}}(t)$ is bounded below by zero in Δ since $S(t), S_F(t) \geq 0$ in Δ , and so by the monotone convergence theorem, $\lim_{t \rightarrow \infty} S_{\text{tot}}(t) = L$ for some constant $L \geq 0$, and so $\lim_{t \rightarrow \infty} dS_{\text{tot}}/dt = 0$.

By (2.28), dS_{tot}/dt can converge to zero as $t \rightarrow \infty$ in only three cases: either (a) $S_{\text{eff}} \rightarrow 0$, or (b) $I \rightarrow 0$, or (c) both as $t \rightarrow \infty$.

In cases (b) and (c), $\lim_{t \rightarrow \infty} I = 0$, and so we can proceed to the next part of this proof (showing that all initial states in the disease-free set \mathcal{C} are attracted to the disease- and fear-free set \mathcal{E}).

In case (a), $\lim_{t \rightarrow \infty} S_{\text{eff}} = 0$, but since $S_{\text{eff}} = S + S_F$ for $S, S_F \geq 0$, it must be the case that $\lim_{t \rightarrow \infty} S(t) = 0$ and $\lim_{t \rightarrow \infty} S_F(t) = 0$. Thus,

$$\lim_{t \rightarrow \infty} \frac{dI}{dt} = -\gamma I, \quad (2.29)$$

which means that eventually $I(t) \sim e^{-\gamma t}$, which converges to zero as $t \rightarrow \infty$. Thus, even in this case, $\lim_{t \rightarrow \infty} I = 0$.

Thus, all initial states in Δ are attracted to its subset \mathcal{C} . Moreover, \mathcal{C} is a closed set (in the relative topology) since it is the intersection of the plane $I = 0$ (closed in \mathbb{R}^3 with the standard topology) and Δ . The set \mathcal{C} is also invariant since, if $I = 0$, then $dI/dt = 0$. Thus, \mathcal{C} is a closed invariant set, and so trajectories cannot escape this globally attracting set.

²For a formal statement of the relevant theorem, see theorem 2 in appendix A.

In addition, since the all initial states tend to a disease-free state, the final size of an epidemic, $R_\infty \stackrel{\text{def}}{=} \lim_{t \rightarrow \infty} R(t)$, is well-defined.

Now consider any initial point in \mathcal{C} , *i.e.*, where $I(0) = 0$. In this case,

$$\frac{dS_F}{dt} = -\gamma_F S_F, \quad (2.30)$$

which can be solved for

$$S_F(t) = S_{F0} e^{-\gamma_F t}, \quad (2.31)$$

for any $0 \leq S_{F0} \leq 1$, and so $\lim_{t \rightarrow \infty} S_F(t) = 0$ in $\mathcal{C} \subset \Delta$. As a result, all initial states in \mathcal{C} are attracted to its subset \mathcal{E} .

Moreover, the set \mathcal{E} is closed with respect to the relative topology since it is the intersection of the line $S_F, I = 0$ (closed in \mathbb{R}^3 with the standard topology) and Δ . The set \mathcal{E} is invariant since it is the set of equilibria of the system (2.11). Therefore, the set \mathcal{E} is a closed invariant subset of \mathcal{C} that is globally attracting with respect to \mathcal{C} .

Lastly, by (2.12), $S(t) = 1 - S_F(t) - I(t) - R(t)$, and so

$$\lim_{t \rightarrow \infty} S(t) = 1 - R_\infty = S_\infty. \quad (2.32)$$

Therefore, since all initial states in Δ are attracted to \mathcal{C} , all initial states in \mathcal{C} are attracted to \mathcal{E} , and solution trajectories $\phi(t) = (S(t), S_F(t), I(t))$ are continuous³, \mathcal{E} is a closed invariant set that is globally attracting with respect to Δ .

In other words, every initial state in Δ converges to some disease- and fear-free equilibrium of the form $(S_\infty, 0, 0)$, where $0 \leq S_\infty \leq 1$. □

2.3 The Behavioural SIR with Prevalence- and Fear-Based Fear (bSIR-PF)

In the first behavioural model, fear can only be transmitted to susceptible individuals through their interaction with infected people. However, it is also possible that fear

³The differential equations given in (2.11) are C^∞ .

itself spreads fear: if a susceptible individual interacts with a person who is scared of the disease, they may become scared themselves.

In order to incorporate fear-based spread of fear into the existing behavioural SIR model (the bSIR-P model), it is assumed that susceptible individuals can additionally become fearful through contact with fearful individuals at a reduced “fear transmission” rate of $r_{\beta_F} \beta_F$, where r_β is the ***proportion of the full fear transmission rate for fear-based spread of fear***. We require that $0 < r_{\beta_F} \leq 1$ since we assume that susceptible individuals become fearful by interacting with fearful people more slowly than when they interact with infected people; a second-hand account of disease symptoms is likely to be less compelling than a first-hand experience⁴. (Here, we assume that the basis of fear is real, though one could consider the case where fear of the disease is more compelling than the disease itself by taking $r_{\beta_F} > 1$).

This model is referred to as the “bSIR-PF” model (behavioural SIR with Prevalence-and Fear-based spread of fear). Like the bSIR-P model, the bSIR-PF model is similar to Model III presented in [19], in that the only difference is again in the interpretation of “healthy” individuals.

Note that, in implementing fear-based spread of fear into the model, we have not altered any other processes. In particular, the recovery from fear process still only involves fearful individuals interacting with “healthy” individuals (defined as those who are not infected). But fearful individuals also count as healthy in this model, which would mean that interaction between fearful individuals contributes to the *recovery* from fear. While this may seem inappropriate given that fear helps spread fear, it can be justified as follows: becoming fearful is not inherently risky to an individual (in fact, it should reduce their risk of becoming infected) but recovering from fear could be risky if the infection has not yet gone extinct. Thus, when recovering from fear, an individual might want to be certain that disease prevalence is low. As a result, they might only rely on what they experience first-hand, *i.e.*, witnessing an absence of infected individuals.

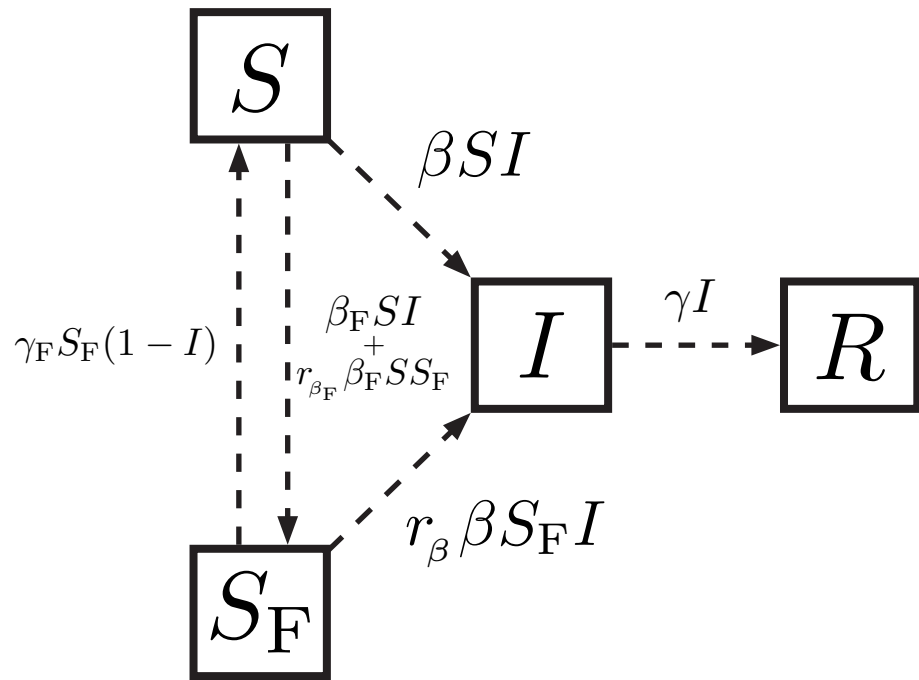


Figure 2.3: A flow chart of the bSIR-PF model, where, in addition to the state variables and parameters from the bSIR-P model, r_{β_F} is the proportion of the full fear transmission rate, β_F , used for transmission of fear by interaction with fearful individuals.

2.3.1 Equations

A flow chart of the bSIR-PF model is given in figure 2.3, and the associated system of ODEs can be written as follows:

$$\frac{dS}{dt} = \gamma_F S_F (1 - I) - \beta SI - \beta_F SI - r_{\beta_F} \beta_F S S_F, \quad (2.33a)$$

$$\frac{dS_F}{dt} = \beta_F SI + r_{\beta_F} \beta_F S S_F - r_\beta \beta S_F I - \gamma_F S_F (1 - I), \quad (2.33b)$$

$$\frac{dI}{dt} = \beta SI + r_\beta \beta S_F I - \gamma I, \quad (2.33c)$$

$$\frac{dR}{dt} = \gamma I. \quad (2.33d)$$

Since only the transmission of fear process has been modified between this model and the bSIR-P model, there are many identical results between the two. Just as with the bSIR-P model, the first three equations do not depend on the state variable R , and the population is assumed to be closed (disease and fear dynamics are assumed to occur on a much faster timescale than vital dynamics), so equation (2.33d) is redundant.

2.3.2 Assumptions

The bSIR-PF model inherits all assumptions from the bSIR-P model, in addition to the following:

- A12.** Fear also spreads to susceptible individuals by contact with those fearful of the disease (fearful susceptibles) through frequency-dependent transmission at a reduced fear transmission rate (provided $r_{\beta_F} \neq 1$). If $r_{\beta_F} = 1$, fear spreads to susceptible individuals at the same rate, regardless of whether they interact with infected or fearful individuals.

⁴We exclude the case where $r_{\beta_F} = 0$ since it would imply that there is no transmission of fear by fearful individuals and so we would be back in the case of the bSIR-P model.

2.3.3 Analysis

One can show that this model is also biologically well-defined through a similar argument as used for the proof of lemma 1. All trajectories starting in Δ will remain in Δ for all times greater than zero.

Adding fear-based spread of fear to the model does not change early epidemic dynamics (when there is no fear) and so the basic reproduction number remains $\mathcal{R}_0 = \beta/\gamma$ for the same reason already stated in section 2.2.3. Moreover, the equation for dI/dt is not changed by the addition of fear-based fear, so any results derived from this equation for the bSIR-P model still hold, including:

1. $\mathcal{R}_0 > 1$ for there to be an epidemic;
2. the effective reproduction number is given by $\mathcal{R}_{\text{eff}} = \mathcal{R}_0 S_{\text{eff}}$;
3. at peak prevalence, $S_{\text{eff}} = S + r_{\beta} S_F = 1/\mathcal{R}_0$.

Since the fear-spread process can now be independent of infection, an analogous basic reproduction number for fear, denoted \mathcal{R}_0^F , can be derived. This quantity gives the number of people one fearful individual will scare while they are fearful in a population that is wholly susceptible to fear. In the absence of infection, people become scared at a rate $r_{\beta_F} \beta_F$, and they remain scared for a mean “fearful period” of $1/\gamma_F$, so

$$\mathcal{R}_0^F = \frac{r_{\beta_F} \beta_F}{\gamma_F}. \quad (2.34)$$

Equilibria

As with the bSIR-P model, the bSIR-PF model has disease- and fear-free equilibria of the form (2.21). If $I = 0$, then it is still the case that $dI/dt = 0$. However,

$$\frac{dS_F}{dt} = -\frac{dS}{dt} = (r_{\beta_F} \beta_F S - \gamma_F) S_F \quad (2.35a)$$

$$= (\mathcal{R}_0^F S - 1) \gamma_F S_F, \quad (2.35b)$$

so both remaining differential equations are equal to zero when $S = 1/\mathcal{R}_0^F$. However, since $I = 0$, $S + S_F = 1$ and so $S_F = 1 - 1/\mathcal{R}_0^F$. Thus, there is also a **disease-free**,

endemic fear equilibrium, of the form

$$(S(t), S_F(t), I(t)) = (1/\mathcal{R}_0^F, 1 - 1/\mathcal{R}_0^F, 0). \quad (2.36)$$

Moreover, in this case, S_F cannot increase initially unless $dS_F/dt > 0$, *i.e.*, unless $\mathcal{R}_0^F > 1$, and so an outbreak of fear cannot be observed unless $\mathcal{R}_0^F > 1$.

In the case where $I = 0$, the model reduces down to an SIS model (or rather an “ $SS_F S$ ” model) where people are “infected” with fear and then return to being susceptible when they recover. Thus, all of the same dynamics predicted by the SIS model are observed here, including the fact that when $\mathcal{R}_0^F \leq 1$, the **fear-free equilibrium** $(S, S_F) = (S_0, 0)$ is stable, but when $\mathcal{R}_0^F > 1$, the **endemic fear equilibrium** $(S, S_F) = (1/\mathcal{R}_0^F, 1 - 1/\mathcal{R}_0^F)$ is stable [6].

Computing the Jacobian generally, we have that

$$DF_{(S, S_F, I)} = \begin{pmatrix} -\beta I - \beta_F I - r_{\beta_F} \beta_F S_F & \gamma_F (1 - I) - r_{\beta_F} \beta_F S & -\gamma_F S_F - (\beta + \beta_F) S \\ \beta_F I + r_{\beta_F} \beta_F S_F & r_{\beta_F} \beta_F S - r_\beta \beta I - \gamma_F (1 - I) & \beta_F S + (\gamma_F - r_\beta \beta) S_F \\ \beta I & r_\beta \beta I & \beta S + r_\beta \beta S_F - \gamma \end{pmatrix}. \quad (2.37)$$

At the disease- and fear-free equilibria,

$$DF_{(S_0, 0, 0)} = \begin{pmatrix} 0 & \gamma_F - r_{\beta_F} \beta_F S_0 & -(\beta + \beta_F) S_0 \\ 0 & r_{\beta_F} \beta_F S_0 - \gamma_F & \beta_F S_0 \\ 0 & 0 & \beta S_0 - \gamma \end{pmatrix}, \quad (2.38)$$

and so the eigenvalues of the Jacobian are $\lambda_1 = 0$, $\lambda_2 = r_{\beta_F} \beta_F S_0 - \gamma_F$, and $\lambda_3 = \beta S_0 - \gamma$, meaning that the disease- and fear-free equilibria are non-hyperbolic, and so we cannot linearize about them to infer their stability.

At the disease-free, endemic fear equilibrium,

$$DF_{(1/\mathcal{R}_0^F, 1 - 1/\mathcal{R}_0^F, 0)} = \begin{pmatrix} -r_{\beta_F} \beta_F (1 - 1/\mathcal{R}_0^F) & 0 & -\gamma_F (1 - 1/\mathcal{R}_0^F) - (\beta + \beta_F)/\mathcal{R}_0^F \\ r_{\beta_F} \beta_F (1 - 1/\mathcal{R}_0^F) & 0 & \gamma_F/r_{\beta_F} + (\gamma_F - r_\beta \beta)(1 - 1/\mathcal{R}_0^F) \\ 0 & 0 & \beta/\mathcal{R}_0^F + r_\beta \beta (1 - 1/\mathcal{R}_0^F) - \gamma \end{pmatrix}, \quad (2.39)$$

which has eigenvalues $\lambda_1 = 0$, $\lambda_2 = -r_{\beta_F} \beta_F (1 - 1/\mathcal{R}_0^F)$, $\lambda_3 = \beta/\mathcal{R}_0^F + r_\beta \beta (1 - 1/\mathcal{R}_0^F) - \gamma$, and so the disease-free, endemic fear equilibrium is non-hyperbolic as well.

2.4 The Effect of Fear on Prevalence Patterns

The SIR model can only predict two prevalence patterns: no epidemic and a single epidemic [20, Lecture 5]. An example of a predicted single epidemic is shown in figure 2.4.

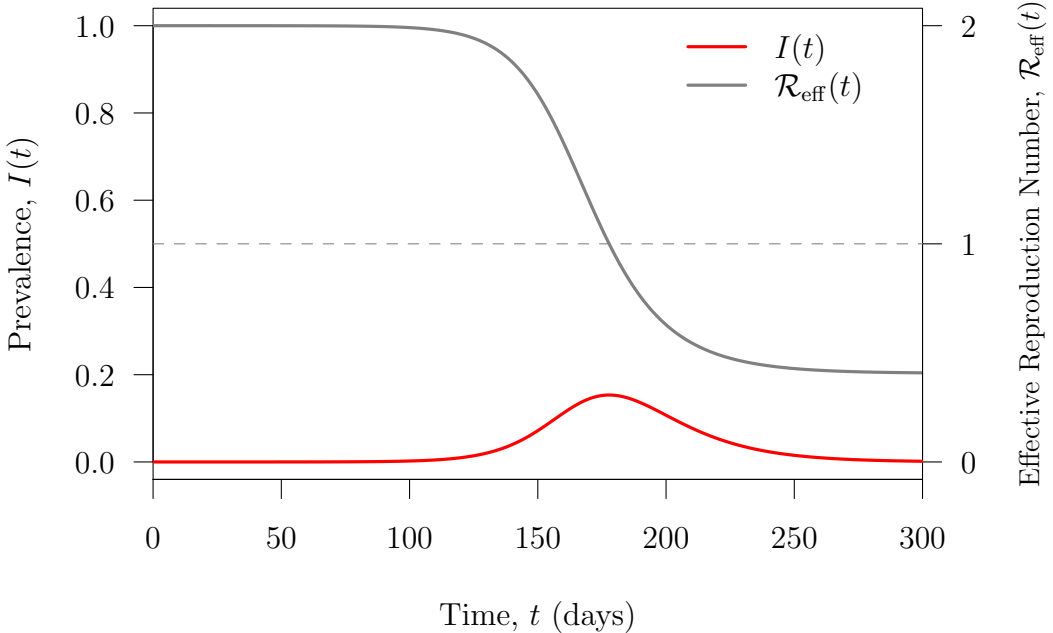


Figure 2.4: A single epidemic predicted by the SIR model. Both the prevalence, $I(t)$, and the effective reproduction number, $\mathcal{R}_{\text{eff}}(t)$, are plotted over time, for $\mathcal{R}_0 = 2$ and $1/\gamma = 10$ days. The epidemic turns over as soon as $\mathcal{R}_{\text{eff}}(t) < 1$.

In both bSIR models, if $\beta \gg \beta_F$, that is, if infection is much faster than the transmission of fear, then the models reduce to the simple SIR with disease transmission rate β and two prevalence patterns: no epidemic and a single epidemic, as shown in figure 2.4. On the other hand, if $\beta_F \gg \beta$, so the transmission of fear is much faster than infection, the models will again reduce to the simple SIR, but this time with the slower disease transmission rate $r_\beta \beta$. Thus, any new dynamical behaviour exhibited by the bSIR models (*i.e.*, behaviour that is not predicted by the standard SIR model) would have to occur when fear and infection operate on comparable timescales.

Indeed, the bSIR models predicts multiple waves of infection in certain regions of parameter space where β and β_F are of comparable magnitude, as shown for the

bSIR-P model in figure 2.5.

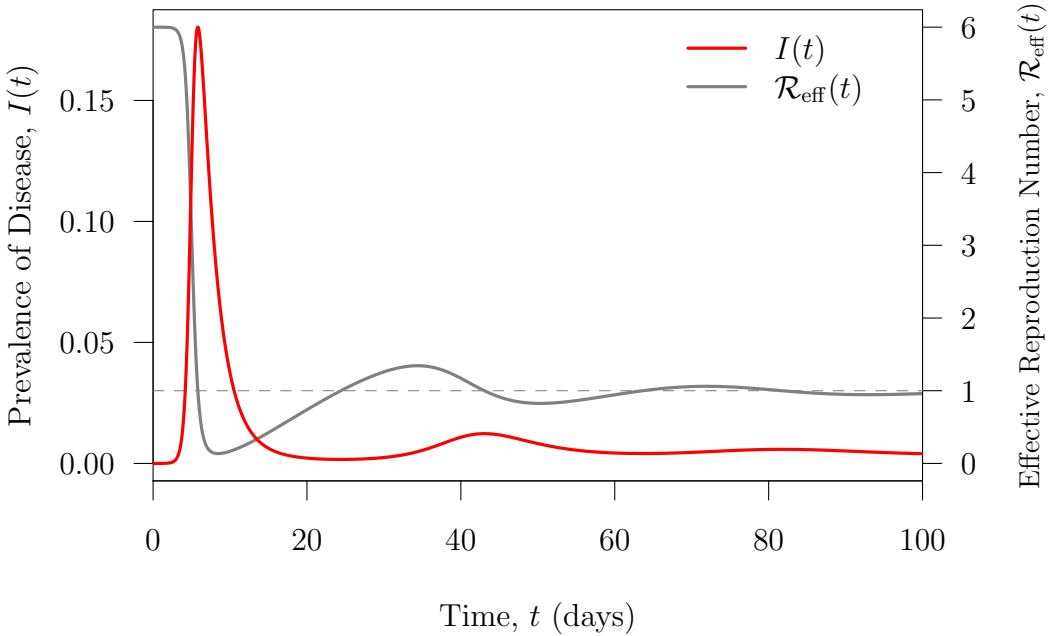


Figure 2.5: Multiple waves of infection predicted by the bSIR-P model. Both the prevalence, $I(t)$, and the effective reproduction number, $\mathcal{R}_{\text{eff}}(t)$, are plotted over time, for $\mathcal{R}_0 = 6$, $1/\gamma = 2$ days, $\beta_F = 6/\text{day}$, $\gamma_F = 0.05/\text{day}$, and $r_\beta = 0$ (perfect quarantine of fearful individuals). The epidemic peaks are precisely when $\mathcal{R}_{\text{eff}}(t) = 1$.

Note that these waves are *not* similar to damped oscillations onto an endemic equilibrium (as can be observed in the SIR model with vital dynamics); these waves are a dynamically distinct pattern that converge to a disease-free state.

The intuition behind the mechanism for multiple waves is rather straight-forward: an epidemic breaks out and, as individuals become infected, they frighten susceptibles who adopt protective measures to reduce their personal risk of becoming infected. As infected individuals recover and the epidemic turns over, fearful susceptibles relax their protective behaviours and are once more at full risk of becoming infected. This built-up store of susceptibles may trigger a subsequent epidemic.

While this intuition is helpful, it is by no means a rigorous explanation of why multiple waves of infection should be predicted by the bSIR-P model; to this end, consider the equation for dI/dt more closely.

Although the bSIR models can exhibit multiple waves of infection while the SIR

model cannot, all of the models ultimately have identical forms for dI/dt in terms of their respective \mathcal{R}_{eff} , as shown already in (2.6) and (2.20). Multiple epidemics require that

$$\frac{dI}{dt} = (\mathcal{R}_{\text{eff}} - 1)\gamma I \quad (2.40)$$

undergoes more than one sign change from positive to negative, *i.e.*, for $\mathcal{R}_{\text{eff}}(t)$, which is always greater than 1 at the beginning of an epidemic⁵, to decrease through 1 more than once.

This behaviour is not possible in the SIR model since $\mathcal{R}_{\text{eff}}(t) = \mathcal{R}_0 S(t)$ and $S(t)$ is monotonically decreasing for all $t \geq 0$. To see that $S(t)$ is monotonically decreasing, recall the equation for dS/dt as given in (2.1a):

$$\frac{dS}{dt} = -\beta SI.$$

Since $\beta > 0$ by assumption, and $S \geq 0$, $I \geq 0 \forall t > 0$ ⁶, $dS/dt \leq 0 \forall t > 0$. Moreover, since each equation in system (2.1) is C^∞ , and thus C^1 , the solution curves $S(t)$ for any initial condition must be continuous. Therefore, since $S(t)$ is a continuous function with non-positive derivative for all $t \geq 0$, $S(t)$ is monotonically decreasing. As a result, $\mathcal{R}_{\text{eff}}(t) = \mathcal{R}_0 S(t)$ is also monotonically decreasing and continuous, with $\mathcal{R}_{\text{eff}}(0) = \mathcal{R}_0 > 1$, so if $\mathcal{R}_{\text{eff}}(t)$ is to decrease below 1, it can only do so once.

On the other hand, multiple waves are entirely possible in the bSIR-model since $\mathcal{R}_{\text{eff}}(t) = \mathcal{R}_0 S_{\text{eff}}(t)$, where $S_{\text{eff}}(t) = S(t) + r_\beta S_{\text{eff}}(t)$. As susceptible individuals become fearful (*i.e.*, they flow from S to S_F), they are “worth less” in the calculation of S_{eff} , as they become discounted by the coefficient r_β . However, when individuals begin recovering from their fear (*i.e.*, they flow from S_F to S), they regain their full value in the calculation of S_{eff} . The larger r_β is, the more pronounced this effect is. As a result, it is entirely possible that $S_{\text{eff}}(t)$, and thus $\mathcal{R}_{\text{eff}}(t)$, is not monotonic, meaning that $\mathcal{R}_{\text{eff}}(t)$ may pass from being greater than 1 to less than 1 multiple times.

Indeed, \mathcal{R}_{eff} is not monotonic in figure 2.5, and thus neither is S_{eff} .

Moreover, if S_F is additionally plotted for this parameter set (see figure 2.6), then it is clear that shortly after the epidemic turns over (just after the first time $\mathcal{R}_{\text{eff}} = 1$), the proportion of fearful individuals begins to decline from its peak (at approximately day 8). The proportion of fearful individuals will decline overall if the rate out of

⁵Recall that $\mathcal{R}_{\text{eff}}(0) = \mathcal{R}_0 > 1$ is required for an epidemic to occur.

⁶Recall that the SIR model is biologically well-defined and so the domain D as given in (2.2) is forward invariant.

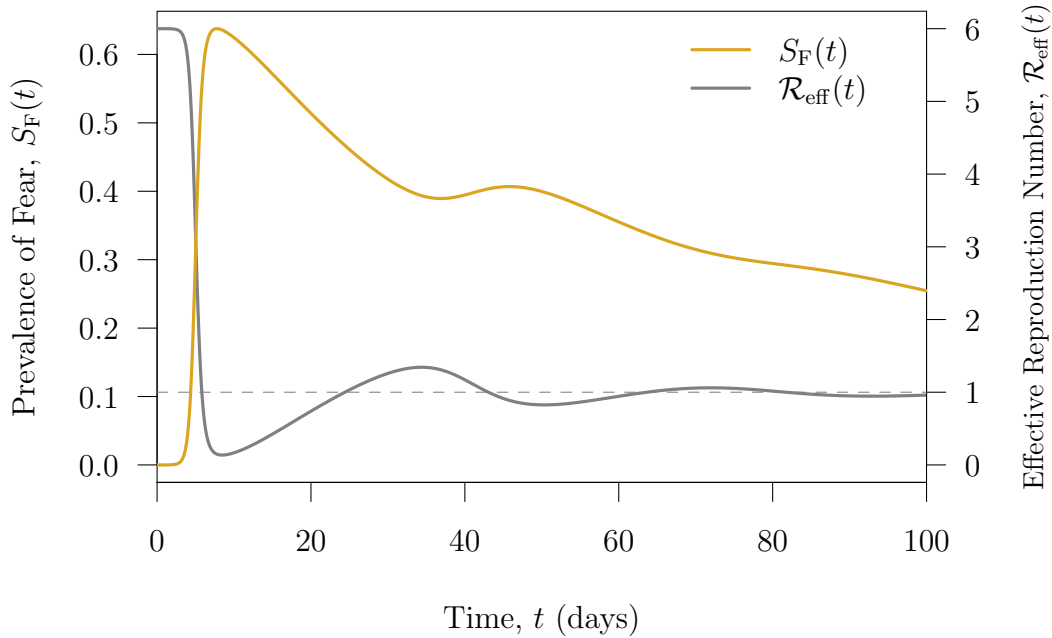


Figure 2.6: Prevalence of fear during multiple waves of infection predicted by the bSIR-P model. Both the prevalence of fear, $S_F(t)$, and the effective reproduction number, $R_{\text{eff}}(t)$, are plotted over time, for the same parameter values as in figure 2.5.

the fearful state exceeds the rate in: that is, fearful individuals are being infected and/or recovering from their fear faster than susceptible individuals are becoming fearful. However, in figure 2.6, $r_\beta = 0$, which means that fearful individuals *cannot* become infected. Instead, the decline in fearful individuals is due to the fact that they are recovering from their fear, and so moving from the S_F state to the S state. In fact, the decline in S_F increases S_{eff} , which in turn increases R_{eff} above 1, meaning that there is again a large enough proportion of susceptible individuals to provoke a second epidemic peak, which occurs the third time $R_{\text{eff}} = 1$. The subsequent waves can be explained with a similar argument.

Chapter 3

Simplifying the bSIR Models

One way that we can begin to understand the dynamical effects of fear in a disease model is by exploring whether it is possible to simplify these behavioural models in any way, and still replicate interesting bSIR dynamics. In this chapter, we consider two ways of simplifying the bSIR models and draw conclusions based on the outcome of these simplifications.

3.1 Basic SIR Fitting

Based on the analysis of both models in chapter 2, there seem to be many parallels between the SIR model (2.1) and the bSIR models (2.11, 2.33). A natural question, then, is whether a more complicated bSIR model can be reduced to a simpler SIR model. In other words, in the case where a bSIR model is more appropriate for the context, we seek to understand whether the SIR model can replicate the bSIR dynamics sufficiently, which would be advantageous since the SIR model has fewer parameters.

As a first step, an SIR model is fitted to simulated bSIR-P prevalence data. We solve the bSIR-P model numerically for six different parameter sets, detailed in table 3.1.

Heuristically, fitting these bSIR data with an SIR model involves the following steps:

1. Choosing SIR parameter values from which to start the search for the bSIR

Parameter Set	\mathcal{R}_0	$1/\gamma$	β_F	γ_F	r_β	I_0	N
1	2	10	0	0.5	0.5	1×10^{-6}	1×10^6
2	2	10	1	0.5	0.5	1×10^{-6}	1×10^6
3	2	10	2.5	0.5	0.5	1×10^{-6}	1×10^6
4	2	10	5	0.5	0.5	1×10^{-6}	1×10^6
5	2	10	3	0.1	0.1	1×10^{-6}	1×10^6
6	2	2	3	0.05	0.1	1×10^{-6}	1×10^6

Table 3.1: A table of parameter values used to simulate the bSIR-P model for fitting with the basic SIR model. The units are as follows: the infectious period, $1/\gamma$, is measured in days, β_F and γ_F are measured in days^{-1} , the population size N is measured in individuals, and all other parameters are dimensionless.

parameters that yield the best fit to the simulated bSIR prevalence data.

- The SIR model has three parameters (β , γ , N). Initial guesses for each are set by choosing the actual β , γ , N values used in simulating the bSIR to generate data.
2. Simulating the SIR model with these starting parameters to get $I(t)$, the prevalence of the disease.
 3. Quantifying how well the simulated SIR data fits the bSIR data.
 - The log-likelihood that the current set of SIR parameters generated the bSIR data “observed” is calculated, giving a sense of how good the fit is. The higher the log-likelihood, the more likely it is that this set of SIR parameters generated the bSIR data (and so the better the fit).
 4. Optimizing the fit.
 - The Nelder-Mead algorithm is used to estimate the maximum likelihood.

The process of fitting arbitrary prevalence data with an SIR model as described above has already been implemented in  through the `fitsir` package [21]. This package is used to generate SIR fits to bSIR prevalence data. We include sample code for this process in appendix B.

The results of fitting are presented in figure 3.1 and table 3.2.

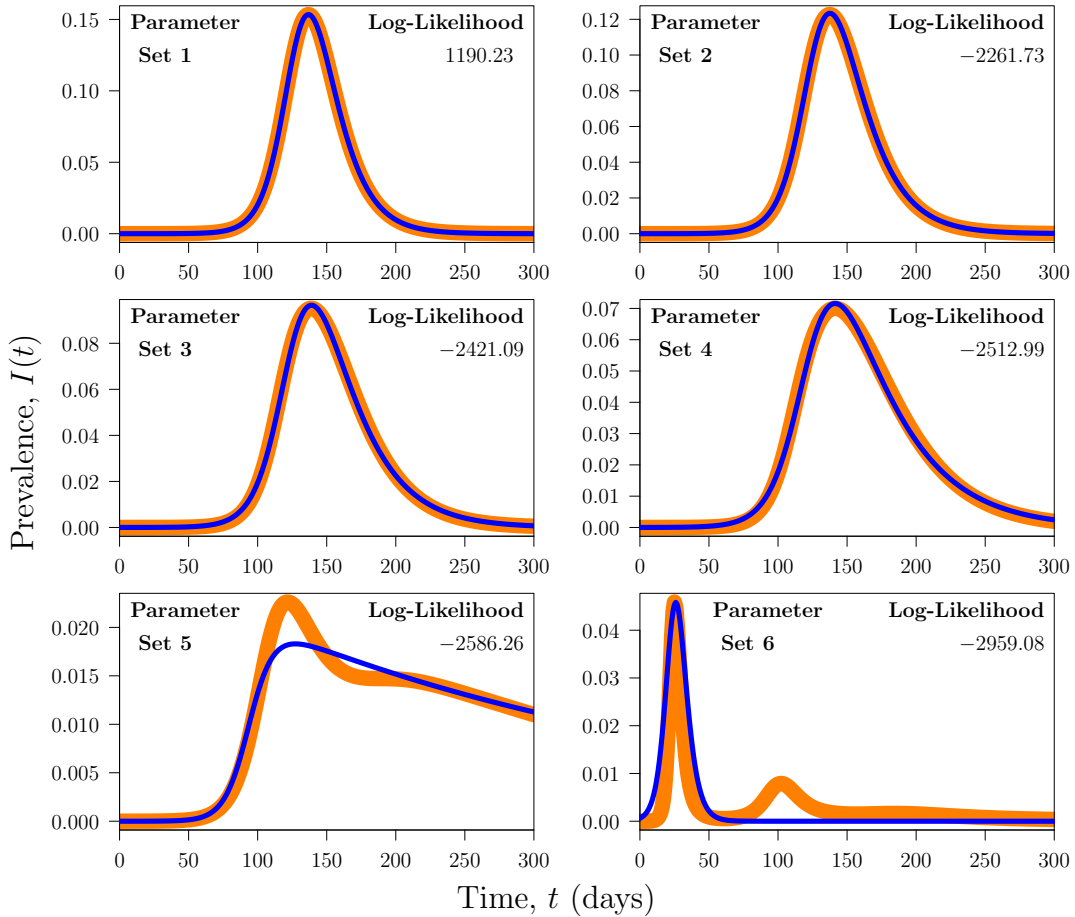


Figure 3.1: Plots of SIR model fits (thinner blue line) to simulated bSIR-P prevalence data (thicker orange line) for each parameter set detailed in table 3.1. The goodness of fit can be evaluated visually by how much these two curves overlap, but more precisely by the log-likelihood value given in each plot. The fitted SIR parameters can be found in table 3.2.

Parameter Set	\mathcal{R}_0	$1/\gamma$	I_0	N
1	2.000	10.000	1.00×10^{-6}	1×10^6
2	2.490	15.686	3.00×10^{-6}	1×10^6
3	3.106	23.812	1.10×10^{-5}	1×10^6
4	3.962	36.716	3.80×10^{-5}	1×10^6
5	38.811	335.532	2.50×10^{-5}	1×10^6
6	1.391	1.758	6.10×10^{-4}	1×10^6

Table 3.2: A table of fitted SIR parameter values corresponding to the bSIR-P parameters in table 3.1. The parameter N is not fitted, but rather fixed before the fitting occurs. The units are as follows: the infectious period, $1/\gamma$, is measured in days, the population size N is measured in individuals, and all other parameters are dimensionless.

In parameter set 1, the transmission rate of fear is $\beta_F = 0$ and so since no one is initially fearful by the assumed initial conditions (2.13), there is no way for individuals to become fearful susceptible. Thus, the bSIR model reduces exactly to an SIR model and so not only should there be a perfect fit with the SIR model, but the fit should also result in identical parameters. Indeed, the shared parameters from rows 1 of tables 3.1 and 3.2 are identical.

The only difference among parameter sets 2-4 is an increasing β_F value. In these sets, the transmission rate of the disease is fixed at $\beta = \mathcal{R}_0\gamma = 0.2/\text{day}$, which is smaller in all three sets than the transmission rate of fear β_F , meaning that fear spreads more quickly than the disease. Here, as β_F increases, the SIR fit gets worse, as reflected in the log-likelihood decreasing. Moreover, all of the fitted parameters increase as fear spreads more quickly.

An observed increase in the fitted parameters can be explained as follows. In the bSIR model, the flow out of the susceptible compartment to the fearful compartment is faster than the flow out of S to I and so, initially, when almost all individuals are susceptible, a larger proportion of the population flows to the fearful state than the infected state. These fearful individuals modify a standard SIR epidemic pattern in two ways: firstly, if they do get infected, they become infected at a reduced transmission rate (reduced by half in this case since $r_\beta = 0.5$), and secondly, if they recover from their fear before they get infected and return to the susceptible class, any subsequent infection of these individuals would be delayed because of the time spent in the fearful susceptible state (which can be thought of as a pseudo-self-quarantine). Both of these changes to a standard SIR epidemic pattern would stretch out the epidemic.

In an effort to compensate for these delays, larger \mathcal{R}_0 and $1/\gamma$ values are observed for the SIR model. To understand this effect, note that the initial growth rate of an epidemic in the SIR model is given by $\gamma(\mathcal{R}_0 - 1)$ [20, Lecture 4]. All else being equal, a larger \mathcal{R}_0 value would lead to a faster initial growth rate. However, $1/\gamma$ is simultaneously increasing, and more quickly than \mathcal{R}_0 , meaning that γ decreases faster than \mathcal{R}_0 increases. As a result the initial growth rate decreases overall¹. Provided a smaller initial growth rate is correlated with a longer epidemic length, this observed effect in the fitted SIR parameters would lead to a prolonged SIR epidemic, which compensates for the delayed infection of fearful individuals in the bSIR epidemic. However, this compensation can only go so far as fear spread becomes faster than infection, which is apparent from the fact that the SIR fit becomes worse.

In parameter set 5, it is still the case that $\beta = 0.2/\text{day} > \beta_F = 3/\text{day}$, but γ_F and r_β are both much smaller, which means that fearful individuals both recover from their fear and get infected at much slower rates. In other words, the flow out of the S_F compartment is much slower than the flow in. Combined with the fact that susceptibles become fearful faster than they become infected, the pseudo-self-quarantine effect of the fearful susceptible compartment is more pronounced, stretching out the epidemic even more drastically than with previous parameter sets, and creating two waves of infection (the second of which is harder to distinguish). We observe both a significantly larger \mathcal{R}_0 and $1/\gamma$, though $1/\gamma$ increases much more than \mathcal{R}_0 , which, by the argument above, would significantly prolong the SIR epidemic.

Parameter set 6 was chosen specifically to demonstrate easily-distinguishable multiple waves of infection predicted by the bSIR models. It is not surprising that the SIR fit is the worst here since it is impossible for the SIR model to capture the second wave of infection. The SIR fit is mainly centred on the first epidemic, though the fitted epidemic is wider than the simulated bSIR-P epidemic, presumably in an effort to somewhat capture the second wave. Interestingly, the \mathcal{R}_0 and $1/\gamma$ values for both the fitted and simulated epidemics are rather close to each other, and smaller than the set bSIR values, but the initial proportion of infected individuals is much larger for the fitted epidemic, which may be due to the fit being stretched out by the second wave of infection.

Although, as expected, the SIR model cannot replicate all bSIR dynamics (namely, the most interesting prevalence pattern—multiple waves of infection), the process of fitting a simpler SIR model to a more complicated bSIR did give us more insight into the mechanics of the bSIR model. Mainly, when fear transmits either more slowly or

¹This assertion can be verified through direct calculation using the values of \mathcal{R}_0 and $1/\gamma$ in table 3.2

not much more quickly than the disease, the bSIR dynamics are nearly identical to an SIR model with an increased basic reproduction number and a prolonged infectious period. Thus, if a simple SIR model is being fitted to data where individuals adopt protective behaviours due to fear, both the basic reproduction number and the infectious period of the disease may be overestimated.

3.2 Fast-Fear Approximation

Based on the previous section, it seems that when the spread of fear is faster than the spread of the disease, it is more difficult to fit an SIR model well to simulated bSIR data. As a result, let us consider the fast-fear case more closely.

Here, we assume that fear processes occur on a faster timescale than disease processes to derive the following approximation [B. Bolker, pers. comm.].

More precisely, assume that $\min(\beta_F, \gamma_F) \gg \max(\beta, \gamma)$. If fear is much faster than disease, the disease processes can be assumed constant (*i.e.*, in the limit where $\beta, \gamma \rightarrow 0$), which reduces the bSIR-P model to the following subsystem:

$$\frac{dS}{dt} = -\beta_F SI + \gamma_F(1 - I)S_F, \quad (3.1a)$$

$$\frac{dS_F}{dt} = \beta_F SI - \gamma_F(1 - I)S_F. \quad (3.1b)$$

This subsystem is at equilibrium when

$$\beta_F SI - \gamma_F(1 - I)S_F = 0, \quad (3.2a)$$

$$\hat{S}_F = \left(\frac{\beta_F I}{\gamma_F(1 - I)} \right) \hat{S}. \quad (3.2b)$$

At equilibrium, the fraction of total susceptibles that are fearful, *i.e.*, the **fraction**

fearful at equilibrium, is given by

$$f = \frac{\hat{S}_F}{S_{\text{tot}}} = \frac{\hat{S}_F}{\hat{S} + \hat{S}_F} \quad (3.3a)$$

$$= \frac{\beta_F I / (\gamma_F(1 - I)) \hat{S}}{\hat{S} + \beta_F I / (\gamma_F(1 - I)) \hat{S}} \quad (3.3b)$$

$$= \frac{\beta_F I / (\gamma_F(1 - I))}{1 + \beta_F I / (\gamma_F(1 - I))} \quad (3.3c)$$

$$= \frac{\beta_F I}{\gamma_F(1 - I) + \beta_F I} \quad (3.3d)$$

$$= \frac{\beta_F I}{\gamma_F + (\beta_F - \gamma_F)I} \quad (3.3e)$$

$$= \frac{I}{\gamma_F/\beta_F + (1 - \gamma_F/\beta_F)I}. \quad (3.3f)$$

The fraction fearful at equilibrium depends only on the state variable I , which is presumed constant on the fast timescale over which fear spreads. We can derive an **effective transmission rate**, β_{eff} , as the weighted average,

$$\beta_{\text{eff}}(I) = \beta[(1 - f(I)) + r_\beta f(I)] = \beta[1 + (r_\beta - 1)f(I)], \quad (3.4)$$

meaning that β_{eff} is a linear transformation of $f(I)$. Now, the full bSIR-P model can be reduced to an SIR model with transmission rate $\beta_{\text{eff}}(I)$:

$$\frac{dS}{dt} = -\beta_{\text{eff}}(I)SI, \quad (3.5a)$$

$$\frac{dI}{dt} = \beta_{\text{eff}}(I)SI - \gamma I. \quad (3.5b)$$

We integrate (3.5) with initial conditions $(S, I)(0) = (1 - 1/N, 1/N)$ to investigate how well the fast-fear approximation captures the dynamics of the full bSIR-P model.

In row 1 of figure 3.2, simulated bSIR-P prevalence data for two parameter sets are plotted with the corresponding SIR model and effective transmission rate $\beta_{\text{eff}}(I)$ from the fast-fear approximation. Both parameter sets feature faster transmission of fear than of disease, so that the fast-fear approximation could potentially provide a good fit.

Despite the fact the both bSIR-P parameter sets used feature faster transmission

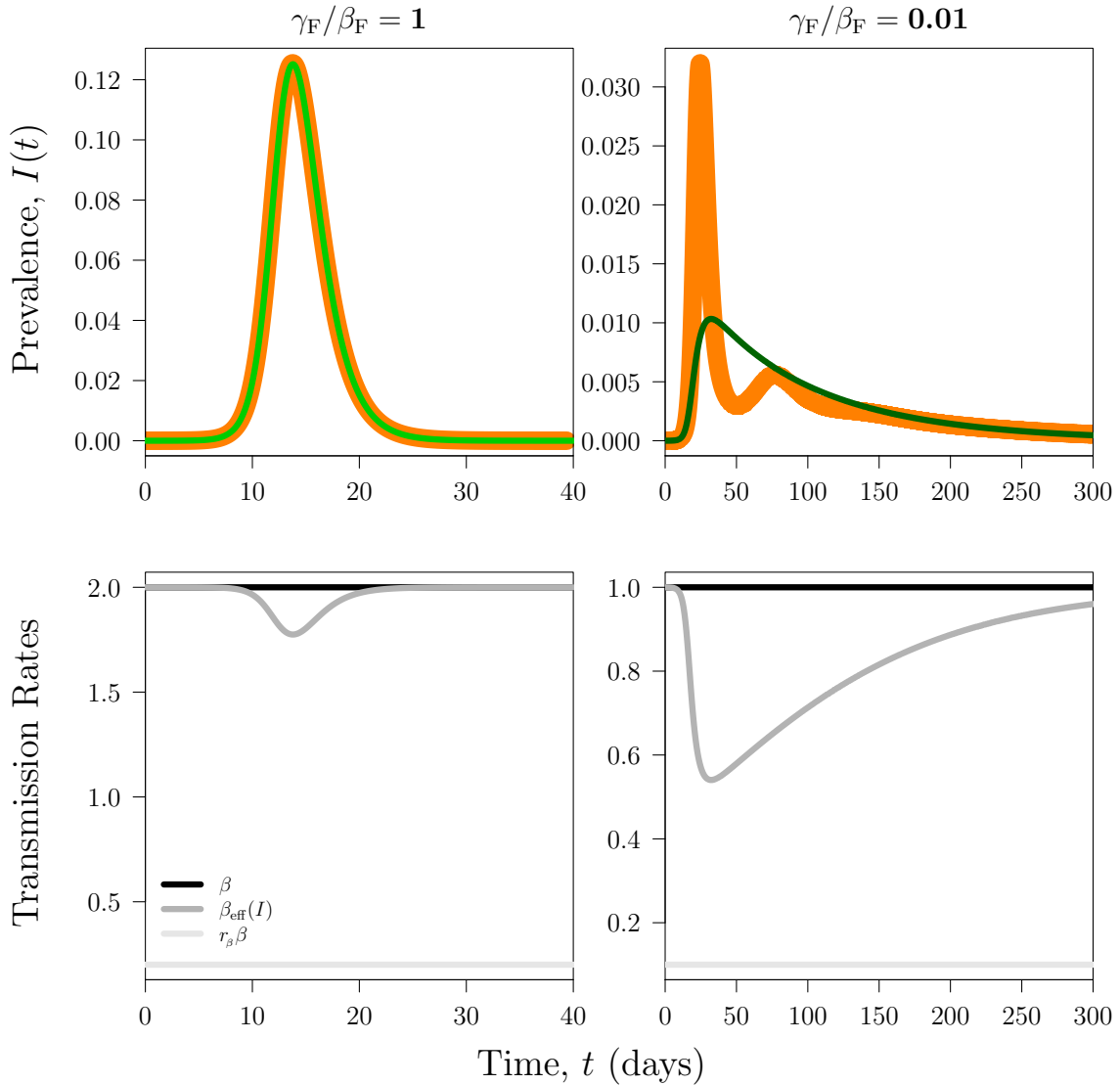


Figure 3.2: Results of fast-fear approximation fits to simulated bSIR-P prevalence data for two different parameter sets (by column) where fear transmits more quickly than disease. Row 1: plots of prevalence curves generated by the SIR model with the fast-fear approximation (thinner green curve) over simulated bSIR-P prevalence data (thicker orange curve). Row 2: plots of relevant transmission rates for each set, including $\beta_{\text{eff}}(I)$, as well as β and $r_\beta \beta$, the upper and lower limits of $\beta_{\text{eff}}(I)$, respectively. The bSIR-P parameters used for column 1 are $\mathcal{R}_0 = 2$, $\gamma = 1/\text{day}$, $r_\beta = 0.1$, $\beta_F = \gamma_F = 10/\text{day}$ and for column 2 are $\mathcal{R}_0 = 2$, $\gamma = 0.5/\text{day}$, $r_\beta = 0.1$, $\beta_F = 3/\text{day}$, $\gamma_F = 0.05/\text{day}$ (the same as parameter set 6 from section 3.1).

of fear than of disease, the fast-fear approximation provides a much better fit to the prevalence curve in column 1 than in column 2. One might expect the fit to be better in column 1, where there is a single epidemic, than in column 2, where there are multiple waves of infection, since the fast-fear approximation fits with an SIR model that is only capable of generating at most one epidemic. However, it is not entirely clear why the fast-fear approximation would not at least provide a good fit for the first epidemic in column 2. To understand why this fit is so poor, let us consider the effective transmission rate $\beta_{\text{eff}}(I)$ being used in the fast-fear approximation more closely.

In row 2 of figure 3.2, the relevant transmission rates for each fast-fear fit are plotted over the same time scale as the corresponding prevalence curve. Both parameter sets feature a dip in $\beta_{\text{eff}}(I)$ around the time of the first epidemic peak. This dip slows down disease transmission so that the epidemic turns over at a lower peak prevalence than it would if the full transmission rate β were used in the SIR model the entire time. This effect mimics the beneficial effects of fear in the bSIR-P model – that is that fear can help decrease peak prevalence because of the protective behaviours frightened individuals adopt.

In column 1, the magnitude of the dip in $\beta_{\text{eff}}(I)$ relative to β and $r_\beta \beta$ seems to be almost perfect since it allows for an excellent fit to the bSIR-P data. In column 2, the magnitude of the dip is very large, leading to a drastic slowdown in disease transmission, to the point where the epidemic is stunted and turns over at a much lower peak prevalence than observed in the bSIR-P data.

The fact that $\beta_{\text{eff}}(I)$ dips much less in column 1 than in column 2 may be somewhat counterintuitive when (3.4) is considered. Since $0 \leq r_\beta \leq 1$ in this model, and $0 \leq f(I) \leq 1$, then $\beta_{\text{eff}}(I) \leq \beta$. Moreover, $f(I)$ is monotonically increasing, which means that $\beta_{\text{eff}}(I)$ is monotonically decreasing in I so as the epidemic takes off, we might expect a dip in $\beta_{\text{eff}}(I)$. However, the prevalences in column 1 are much larger than the prevalences in column 2, and so we might (naively) expect the dip in $\beta_{\text{eff}}(I)$ in column 1 to be larger than the dip in column 2.

However, the magnitude of the dip in $\beta_{\text{eff}}(I)$ is dependent on $f(I)$, which depends on γ_F/β_F . In figure 3.3, $f(I)$ is plotted for the two γ_F/β_F values featured in figure 3.2.

When $\gamma_F/\beta_F = 1$, as in column 1 of figure 3.2, the fraction of fearful susceptibles changes linearly with I . When $\gamma_F/\beta_F = 0.01 < 1$, as in column 2 of the same figure, the fraction fearful changes superlinearly with I , meaning that the proportion fearful will always be larger than the proportion infected. In this case, as I increases

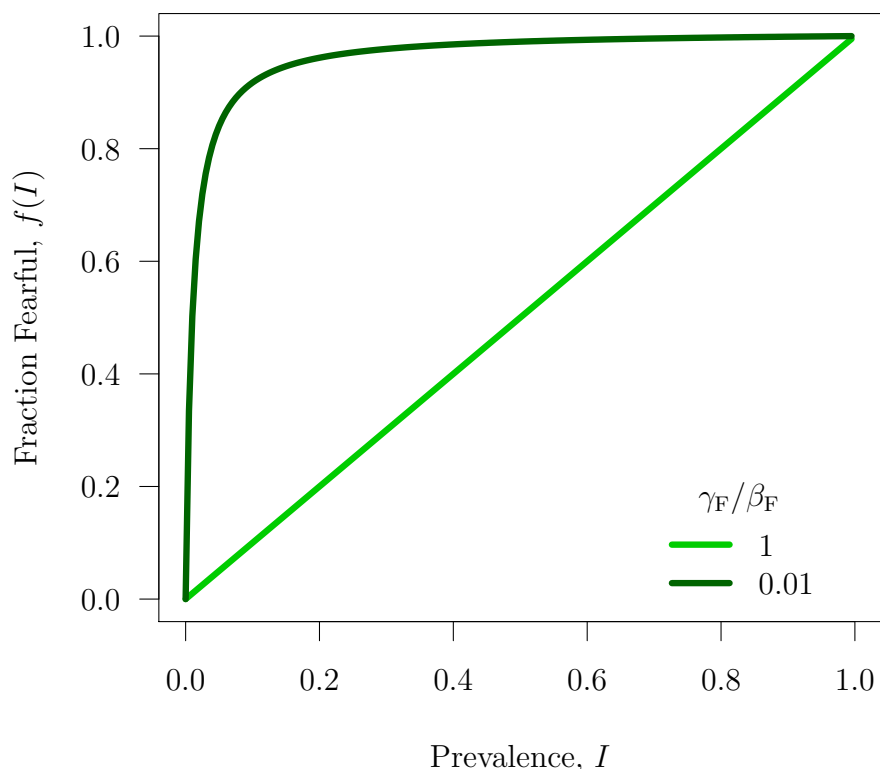


Figure 3.3: A plot of the fraction fearful at the fast-fear equilibrium, f , as a function of prevalence, I , for two values of γ_F/β_F , corresponding to those used in the two columns of 3.2.

from 0, the difference between f and I increases extremely quickly, which leads to a significant dip in $\beta_{\text{eff}}(I)$ at the outset, stalling the epidemic, and generating a bad fit for the bSIR-P data. Thus, when $\gamma_F/\beta_F \ll 1$, $f(I)$ is amplified, leading to a larger magnitude dip in $\beta_{\text{eff}}(I)$, which can create an underestimate of even a small epidemic.

Overall, the success of the fast-fear approximation is not just dependent on the transmission of fear being fast relative to disease, but it is also dependent on the recovery from fear not being too slow relative to its transmission. If recovery from fear is too slow, not only may the bSIR-P model predict multiple waves which cannot be replicated with a standard SIR model, but even the first epidemic may not be fitted well due to the dip in $\beta_{\text{eff}}(I)$ when the epidemic takes off being amplified substantially when $\gamma_F/\beta_F \ll 1$.

Chapter 4

The Effects of Fear on Public Health Metrics

Based on the previous analysis in chapters 2 and 3, it is clear that incorporating fear into the basic SIR model can dramatically change the pattern of prevalence predicted, in a way that cannot be easily simplified. In particular, multiple waves of infection may be observed. As a result, it is not clear how various epidemiological metrics important to public health strategies might change if the prevalence pattern is more complex due to the inclusion of fear.

In this chapter, the effect of fear on three public health metrics is explored in both bSIR models.

1. **Outbreak length (time to extinction):** Minimizing the outbreak length may be favourable (particularly if doing so does not increase the peak prevalence) and so the time to extinction of an epidemic has been studied in a variety of modelling contexts [22–24]. The longer an epidemic persists, the longer resources must be diverted from other health programs to tackle the outbreak at hand. Moreover, giving the pathogen more time in its human host could lead to unfavourable evolution; the pathogen could become more virulent, more transmissible, etc. [25]. Lastly, a longer time to extinction could facilitate the stochastic resurgence and persistence of a disease [23].
2. **The final size of the epidemic:** A priority in public health is to minimize the cumulative case count (final size) of an epidemic and so the final size has also been well-studied in infectious disease modelling [26–29]. All else being equal,

if fewer individuals are affected by the disease, the smaller the socioeconomic cost of the outbreak, and the fewer the public health resources required to bring the outbreak under control.

3. **Peak prevalence of each wave of infection:** It is also favourable to minimize the peak prevalence (that is the number of currently infected individuals at the peak of each epidemic) since it is the maximum number of cases a public health system has to deal at a single point in time during an epidemic. The peak prevalence tests the system's short-term capacity.

We calculate each of these metrics by integrating the model equations numerically with the initial conditions given in (2.13). Sample code for each calculation is included in appendix C.

To consider the effect of fear of the disease on the above three public health metrics, we must first quantify “fear” in the model. There are three model parameters associated with fear: β_F , the transmission rate of fear, γ_F , the recovery rate from fear, and r_β , the proportion of the full transmission rate β that applies to fearful susceptibles.

In the behavioural models, the quantitative effect of fear on disease dynamics is most closely related to the parameter r_β , which is the proportion of the full transmission rate β applied to fearful susceptibles. Unfortunately, this quantity is not easy to interpret. However, note that if $r_\beta = 1$, fear has *no effect* since fearful susceptibles are subject to exactly the same transmission rate as regular susceptibles. On the other hand, if $r_\beta = 0$, fearful susceptibles cannot get infected, and so this parameter value represents fearful individuals subjecting themselves to a perfect self-quarantine, *i.e.*, fear is *perfectly effective*. There is an inverse relationship between r_β and how effective fear is in the model. Thus, we define $1 - r_\beta$ to be the *effectiveness of fear* and consider the public health metrics of interest as functions of this quantity.

As for the remaining two fear parameters, β_F and γ_F , recall from chapter 3 that the relative magnitude of these two parameters can change the prevalence pattern greatly; if $\beta_F > \gamma_F$, multiple waves of infection may be observed due to the pseudo-self-quarantine effect discussed previously. Thus, to explore the effect of fear on these public health metrics, the following three cases should be considered:

1. $\beta_F > \gamma_F$: people become fearful faster than they relax their fear;
2. $\beta_F = \gamma_F$: people become fearful and relax their fear at the same rate;

3. $\beta_F < \gamma_F$: people relax their fear faster than they become fearful.

The goal of this chapter is to systematically explore the effect of fear on public health metrics. However, the latter two cases do not yield unexpected results since fearful is unable to build up, and so only the results of case 1 are presented here in the main text; full results for all cases can be found in appendix D.

Lastly, it is not only important to consider the relative magnitudes of the two rates associated with fear; we must also consider how the disease timescale compares to the timescale upon which fear operates. The following three cases will be considered simultaneously (which makes for nine cases in total):

1. $\beta_F > \beta$: fast fear transmission relative to infection;
2. $\beta_F = \beta$: fear transmission and infection of equal speed;
3. $\beta_F < \beta$: slow fear transmission relative to infection.

In considering the public health metrics of interest as functions of the effectiveness of fear, we will find it useful to know the number of waves of infection for each effectiveness of fear value and combination of other parameters. Sample code for calculating the number of peaks on the prevalence curve can be found in appendix C.3.

4.1 The Behavioural SIR with Prevalence-Based Fear (bSIR-P)

4.1.1 Outbreak Length

Initially, we might expect that as fear becomes more effective, the pseudo-self-quarantine effect is exacerbated, making it easier to build up a store of fearful susceptibles. We would then expect these frightened individuals to eventually trickle back into the fully susceptible state and/or start a new, distinct wave of infection, prolonging the overall outbreak monotonically.

The outbreak length (time to extinction) is computed numerically for three different parameter set types, as discussed in the previous section. Time to extinction is defined as the first time when the proportion infected, $I(t)$ falls below $1/N$, which

is equivalent to less than one individual being infected. Sample code for calculating the time to extinction can be found in appendix [C.4](#).

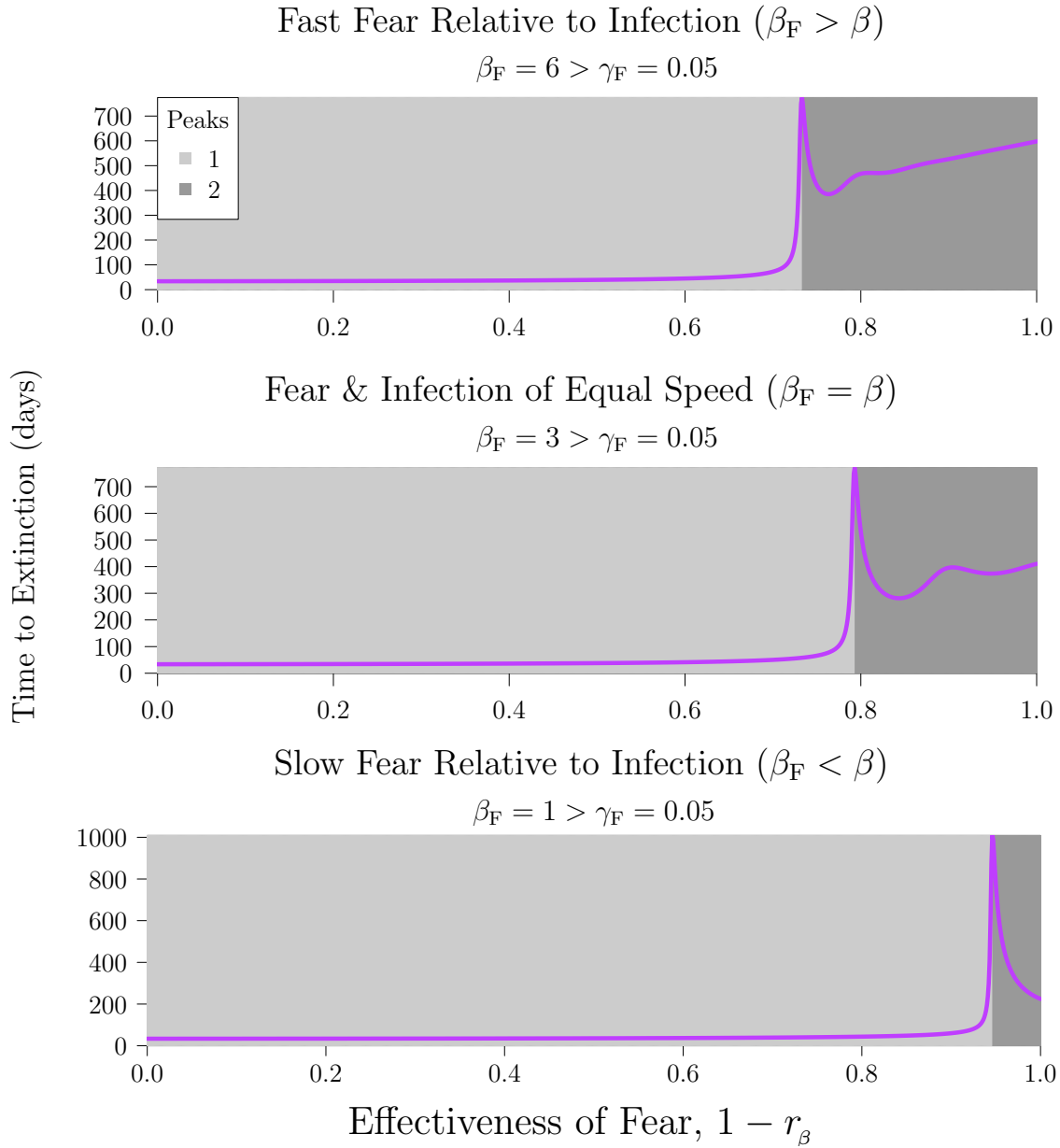


Figure 4.1: Outbreak length (time to extinction) as a function of the effectiveness of fear ($1 - r_\beta$) for three different parameter sets in the bSIR-P model. Infection parameters and the population size are fixed among the plots, with $\mathcal{R}_0 = 6$, $\gamma = 0.5/\text{day}$ (and thus $\beta = \mathcal{R}_0 \cdot \gamma = 3/\text{day}$), and $N = 10^6$ individuals. Fear parameters vary, as given in each plot title. Background shading denotes the number of peaks present in the prevalence curve for each fixed r_β value (and so for each fixed effectiveness of fear value, $1 - r_\beta$).

In analyzing figure 4.1, let us first consider the behaviour of the time to extinction within each panel (as the effectiveness of fear varies), and then among the panels (as the relative transmission speed of fear and infection changes).

Within each panel, as the effectiveness of fear increases, time to extinction is initially constant and then increases dramatically, soaring from below 100 days in all parameter sets to above 700 days, prolonging the epidemic by about two years. This spike peaks near the transition between one wave of infection and two, and then dips steeply, increasing again or oscillating in some cases.

The initial plateau in time to extinction can be explained as follows: when fear is not very effective, the disease transmission rate out of either susceptible compartment is roughly equal. Thus, movement between the susceptible compartments can be ignored; there is effectively no benefit to being fearful at the population level. Since fear does not affect disease transmission, the time to extinction will not change either, and so time to extinction will be an almost constant function of the effectiveness of fear.

To understand the spike and subsequent dip in the time to extinction near the transition between one to two epidemic peaks, consider the proportion susceptible, fearful susceptible and infected over time for effectiveness of fear values just before, exactly at, and just after the threshold and the parameter set in row 1 of figure 4.1 (see figure 4.2). As fear becomes more effective before the threshold (*i.e.*, $1 - r_\beta$ increases just before 0.733), the epidemic is prolonged substantially. However, after the initial epidemic (approximately past day 75), the proportion of susceptibles remains about constant. Any subsequent infection is due to fearful individuals becoming infected directly out of the *fearful* state, and not upon returning to the susceptible state¹. However, at this point, the proportion of infecteds is very low, along with the low value of r_β , and so the force of infection out of the fearful state, $r_\beta \beta I$, is extremely low, leading to a significantly prolonged time to extinction.

Lastly, the post-threshold dip in time to extinction is due to the birth of the second wave of infection. As soon as $1 - r_\beta$ passes this threshold and two distinct waves of infection are created, the store of fearful susceptibles that has been built up after the initial epidemic become infected much more quickly in the secondary epidemic, decreasing the time to extinction. However, as the effectiveness of fear increases to 1, the time to extinction increases again since the store of fearful susceptibles is larger, which enables for a larger (and thus longer) secondary epidemic.

¹Fearful individuals do not return back to the susceptible compartment and then become infected as one might expect since recovery from fear is too slow for this set of parameters.

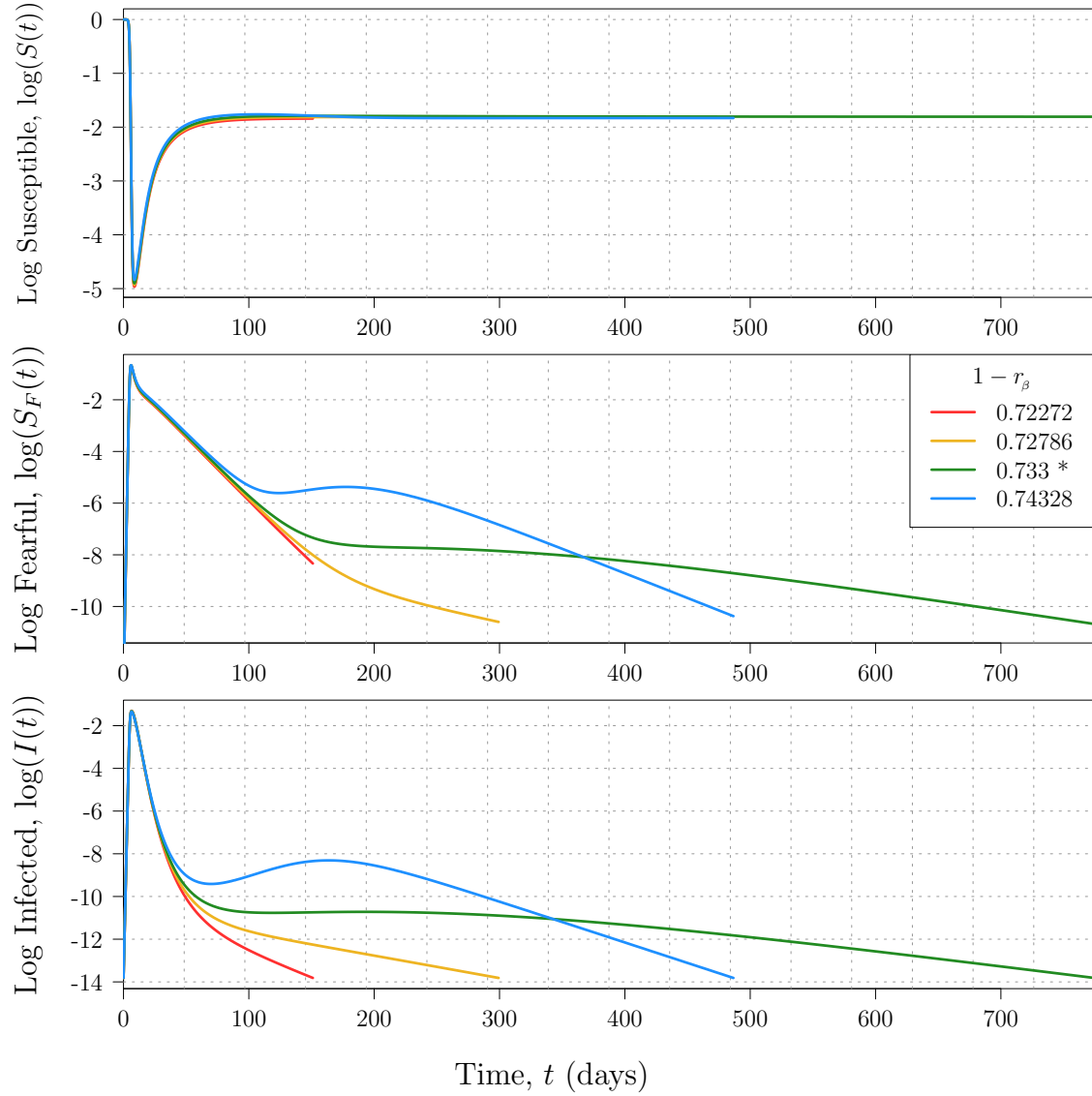


Figure 4.2: The proportion of susceptibles, $S(t)$, fearful susceptibles $S_F(t)$, and infected individuals $I(t)$ over time for values of the effectiveness of fear $1 - r_\beta$ near the threshold between one and two waves of infection in the bSIR-P model. The value of $1 - r_\beta$ exactly at the threshold is marked with an asterisk in the legend. State variables are plotted on a logarithmic scale to more clearly display any oscillatory behaviour. The curves are plotted until the time at which $I(t) < 1/N$. Parameter values for this plot correspond to those used in row 1 of figure 4.1.

Finally, among the three panels of figure 4.1, as fear becomes slower relative to infection, the non-monotonic behaviour that we observe near the transition between one peak and two only occurs for increasingly large values of the effectiveness of fear because the transition itself follows the same pattern. This trend is due to the fact that all susceptibles start off as fully susceptible, and so as fear becomes slower relative to infection, the majority of individuals that leave the susceptible class will be doing so via infection. Thus, a store of frightened susceptibles for a second epidemic becomes more difficult to build up – that is, unless fear is very effective at protecting individuals from infection.

4.1.2 Final Size

Initially, we might expect that as fear becomes more effective, the final size will decrease monotonically. Fearful individuals can only become infected more slowly and so fewer susceptible individuals might become infected as a result of fear. However, in light of the results from section 4.1.1, namely that fear can dramatically prolongue the epidemic, one might instead expect the final size to *increase* when the time to extinction is increased; the longer the epidemic, the larger the number of cases.

We compute the final size numerically for the same three parameter sets as in figure 4.1. The final size is defined as the cumulative case count at the first time when the proportion infected, $I(t)$ falls below $1/N$ (*i.e.*, at the time of extinction). Sample code calculating the final size can be found in appendix C.5.

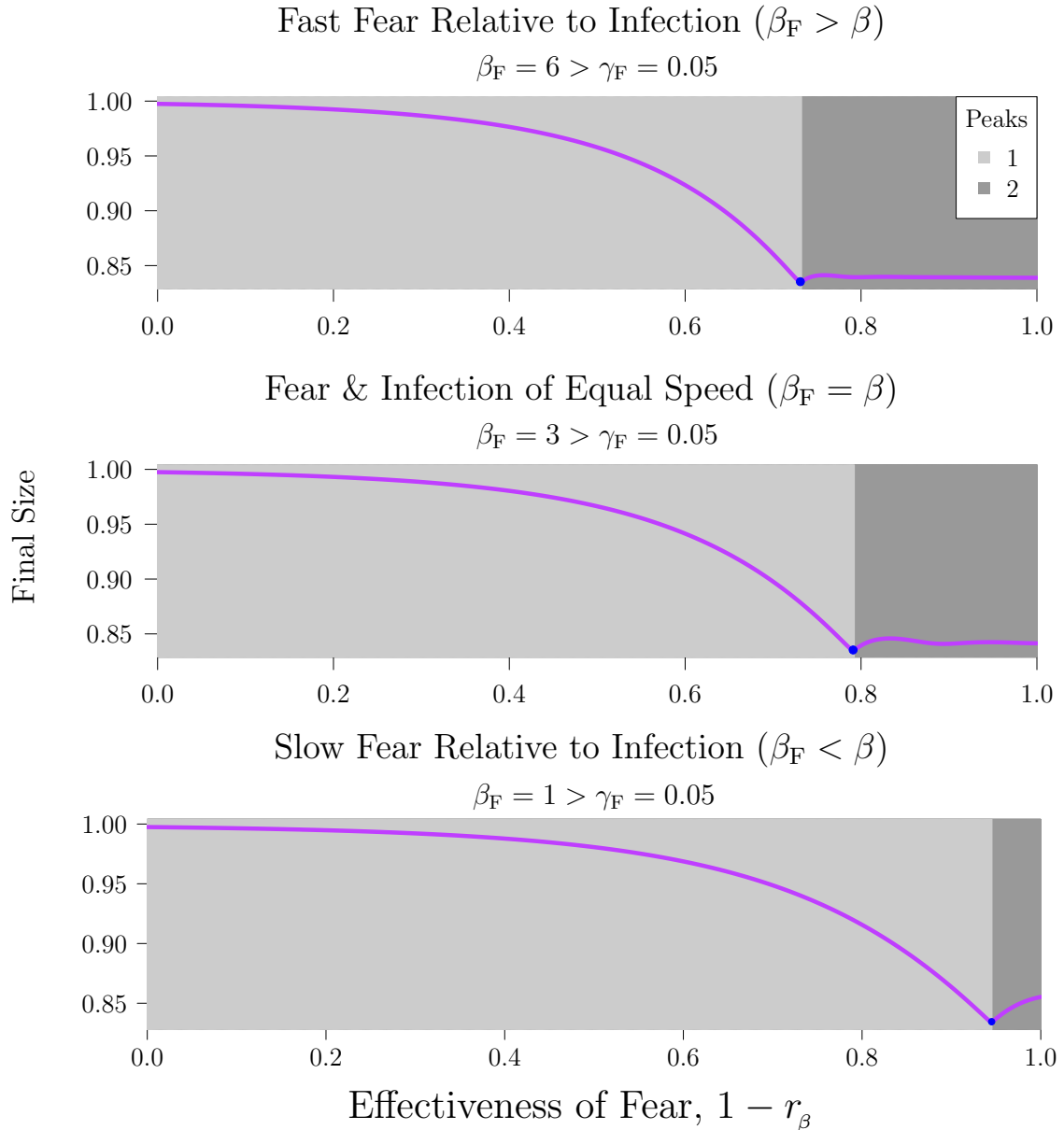


Figure 4.3: Final size as a function of the effectiveness of fear ($1 - r_\beta$) for three different parameter sets in the bSIR-P model. Parameter values are the same as in figure 4.1. The minimum final size is indicated by a blue point.

Again, we first compare the behaviour of the final size within each panel, then among panels.

Within each panel, the final size decreases monotonically until the system transitions from one wave of infection to two, and so a longer time to extinction does not increase the final size as may have been expected. When the final size is decreasing monotonically, it is because many individuals are becoming frightened and their infection contributes to the first (and only) epidemic steadily; however, as effectiveness of fear increases, fewer frightened individuals become infected, decreasing the final size.

It turns out that the minimal final size occurs near the threshold effectiveness of fear (and not when fear is most effective at $1 - r_\beta = 1$). As soon as a second wave of infection appears, the final size increases (at least slightly). It seems that a second epidemic enables the infection of susceptibles that would otherwise escape the disease, thus increasing the final size somewhat.

Among the panels, the pattern is rather similar, although as fear becomes more slow relative to infection, the relationship between final size and the effectiveness of fear approaches being fully monotonically decreasing, since the second wave of infection becomes more difficult to trigger. However, it is also interesting that as the transmission of fear becomes slow relative to infection (that is, as we move down the column of plots), the peak after the minimal final size increases.

4.1.3 Peak Prevalences

As with the final size, one might expect that as fear becomes more effective, peak prevalence decreases since fearful individuals get infected more slowly, possibly leading to fewer infecteds overall (and so in particular at the peak of the epidemic).

We calculate the peak prevalence of each epidemic numerically for the same three parameter sets as in figure 4.1. The peak prevalence is defined as prevalence when $dI/dt = 0$ going from positive to negative (*i.e.*, at each local maximum). Sample code for calculating the peak prevalence can be found in appendix C.6.

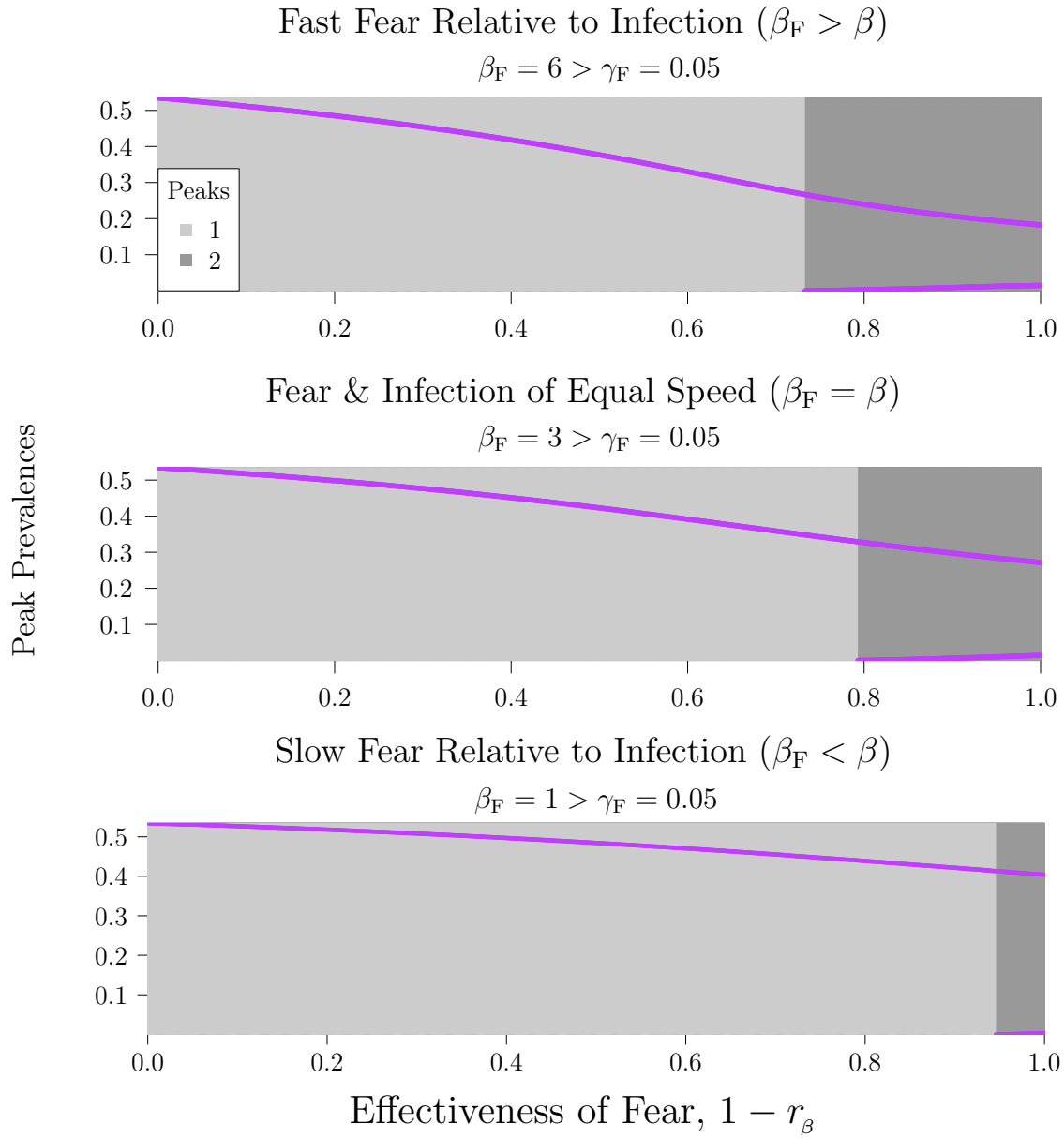


Figure 4.4: Peak prevalence of each epidemic as a function of the effectiveness of fear ($1 - r_\beta$) for three different parameter sets in the bSIR-P model. Parameter values are the same as in figure 4.1.

Unlike in the case of the time to extinction or the final size, the relationship between peak prevalence and the effectiveness of fear is nearly exactly what was predicted. The prevalence at the first peak decreases monotonically. However, the prevalence of the second peak increases slightly as fear becomes more effective. In this case, when fear is very effective, it is easier to build up a store of frightened susceptibles that trigger a larger second epidemic (which is also what leads to a slightly increased final size from its minimum at the threshold in $1 - r_\beta$ for a second epidemic).

4.2 The Behavioural SIR with Prevalence- and Fear-Based Fear (bSIR-PF)

The analysis from the previous section is repeated for the model with both prevalence- and fear-based fear spread (the bSIR-PF model). We use the same parameter sets as in the previous section to allow for comparison between the results of the two models, so that we may explore how the addition of fear-based fear spread changes the resultant pattern. Throughout this section, we assume that the transmission of fear by interaction with fearful individuals occurs at a rate $1/5^{\text{th}}$ the speed of the transmission of fear by interaction with infected individuals (*i.e.*, $r_{\beta_F} = 0.2$).

4.2.1 Outbreak Length

Figure 4.5 shows the outbreak length as a function of the effectiveness of fear in the bSIR-PF model for the case where the transmission of fear is fast relative to recovery from fear. This figure is analogous to figure 4.1 for the bSIR-P model.

When fear transmission is fast relative to disease transmission (rows 1 and 2 of figure 4.5), or when they are of comparable speed, there is a mild increase then decrease in the time to extinction as fear becomes more effective. The fact that the maximum time to extinction occurs at an intermediate value for the effectiveness of fear can be explained with the help of figure 4.6.

When fear is not very effective ($1 - r_\beta = 0.4$), as the epidemic takes off, the proportion of infected people increases, which leads to an increase in the proportion of fearful individuals. However, fear drives fear in this model, and so more individuals become fearful than would if fear were only transmitted by interaction with infected individuals (such as in the bSIR-P model). Since fear is not very effective, fearful

individuals help contribute to a larger overall epidemic, which then burns out more quickly as individuals recover from both the disease and fear. However, since the main epidemic burns out more quickly, there is a larger proportion of fearful susceptibles who do not return to the fully susceptible state in time to sustain the infection, since the recovery from fear occurs at too slow of a rate.

When fear becomes more effective, specifically at the value that leads to the maximal time to extinction ($1 - r_\beta = 0.843$), the proportion of fearful individuals increases as the epidemic increases, but then as the epidemic turns over (approximately at day 6), the proportion of fearful individuals decreases very slowly, despite the fact that the proportion of susceptible individuals continues to decrease significantly. These susceptible individuals are becoming both infected and frightened, but they are becoming frightened more quickly for two reasons. Firstly, fear is assumed to be faster than infection in this case. Secondly, there are more fearful individuals than infecteds at this point in time (as the epidemic turns over at approximately day 6) and both fear and infection contribute to further fear, while only infection contributes to further infection. The very slow *decrease* in the proportion of frightened individuals over this period (as opposed to the increase one would expect due to the influx of susceptibles) is due to the fact that the rate out of the fearful compartment (only via transmission of the disease since recovery from fear is slow) is only slightly faster than the rate in (from the infection of susceptible individuals with fear). In other words, the infection of fearful individuals with the disease continues slowly after the epidemic peak, but at a rate that is slightly faster than the rate at which susceptible individuals are being frightened. This process sustains the infection for a longer time, leading to a longer time to extinction.

However, if fear is perfectly effective, the rate out of the fearful compartment cannot become only slightly faster than the rate into this same compartment after the epidemic peak since the rate out is always zero. Therefore, the infection cannot be sustained by fearful individuals for a longer period of time as in the previous case. Instead, fearful susceptibles remain in this state until they recover from their fear. Since recovery from fear is relatively slow compared transmission of both fear and the disease, these fearful individuals do not return to the susceptible compartment in time to contribute to any epidemic, leading to a smaller, faster epidemic overall.

In the case where fear transmission is slow relative to infection (row 3 of figure 4.5), a similar pattern is observed as in the same case with the bSIR-P model (see figure 4.1). However, in the bSIR-PF model, the spike near the transition between one and two waves of infection is lower than with the bSIR-P model. Recall that the spike in the time to extinction with the bSIR-P model is due to the epidemic

being sustained by frightened individuals at low levels for a long period of time. In the bSIR-PF model, it is still the case that fearful individuals are sustaining the infection, but not for as long of a period of time; there is a larger store of frightened individuals built up since fear is self-reinforcing, leading to a faster second wave of infection and so a faster end to the overall outbreak.

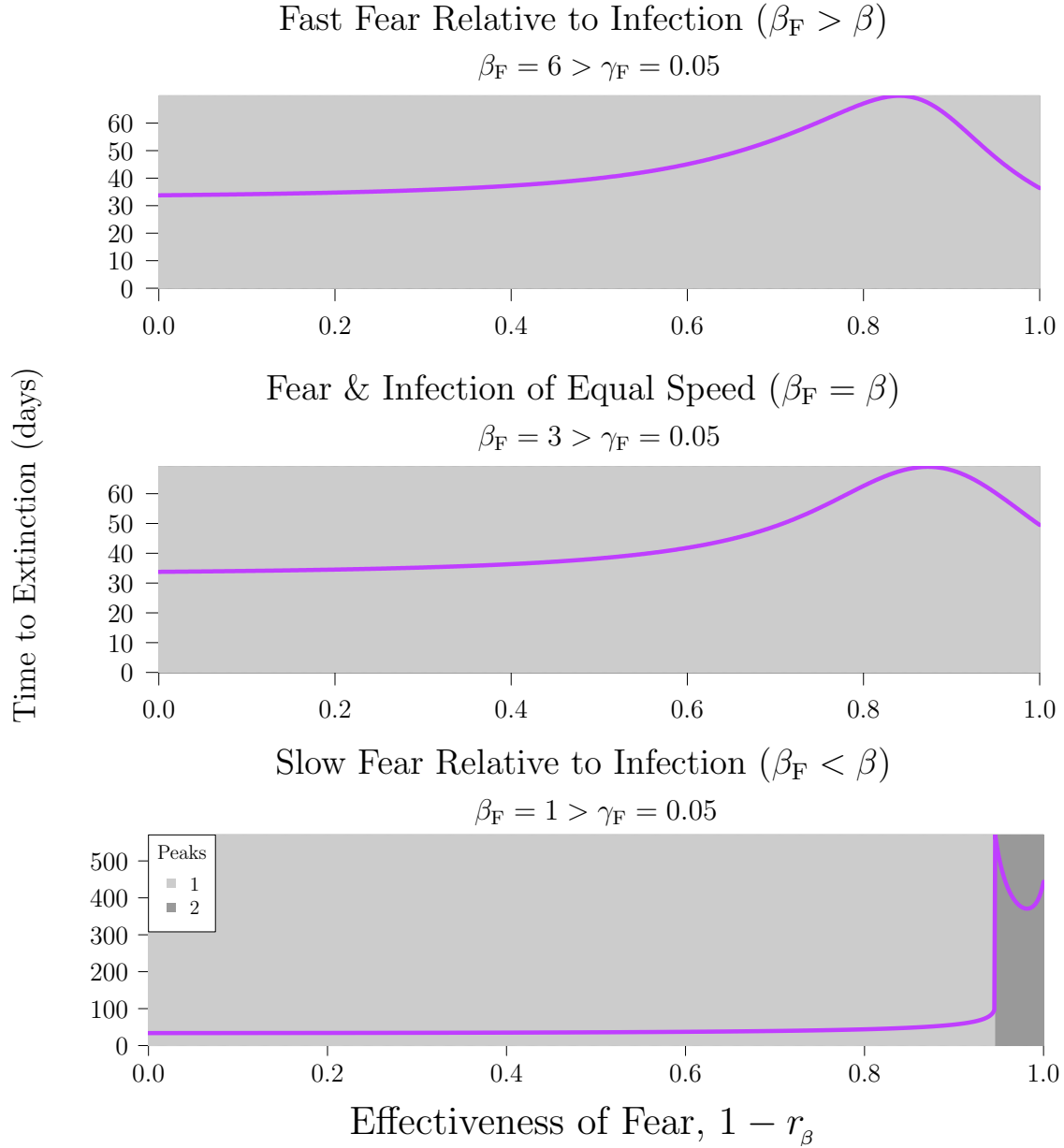


Figure 4.5: Outbreak length (time to extinction) as a function of the effectiveness of fear ($1 - r_\beta$) for three different parameter sets in the bSIR-PF model. This figure is analogous to figure 4.1 for the bSIR-P model, and so parameters are shared in addition to $r_{\beta_F} = 0.2$.

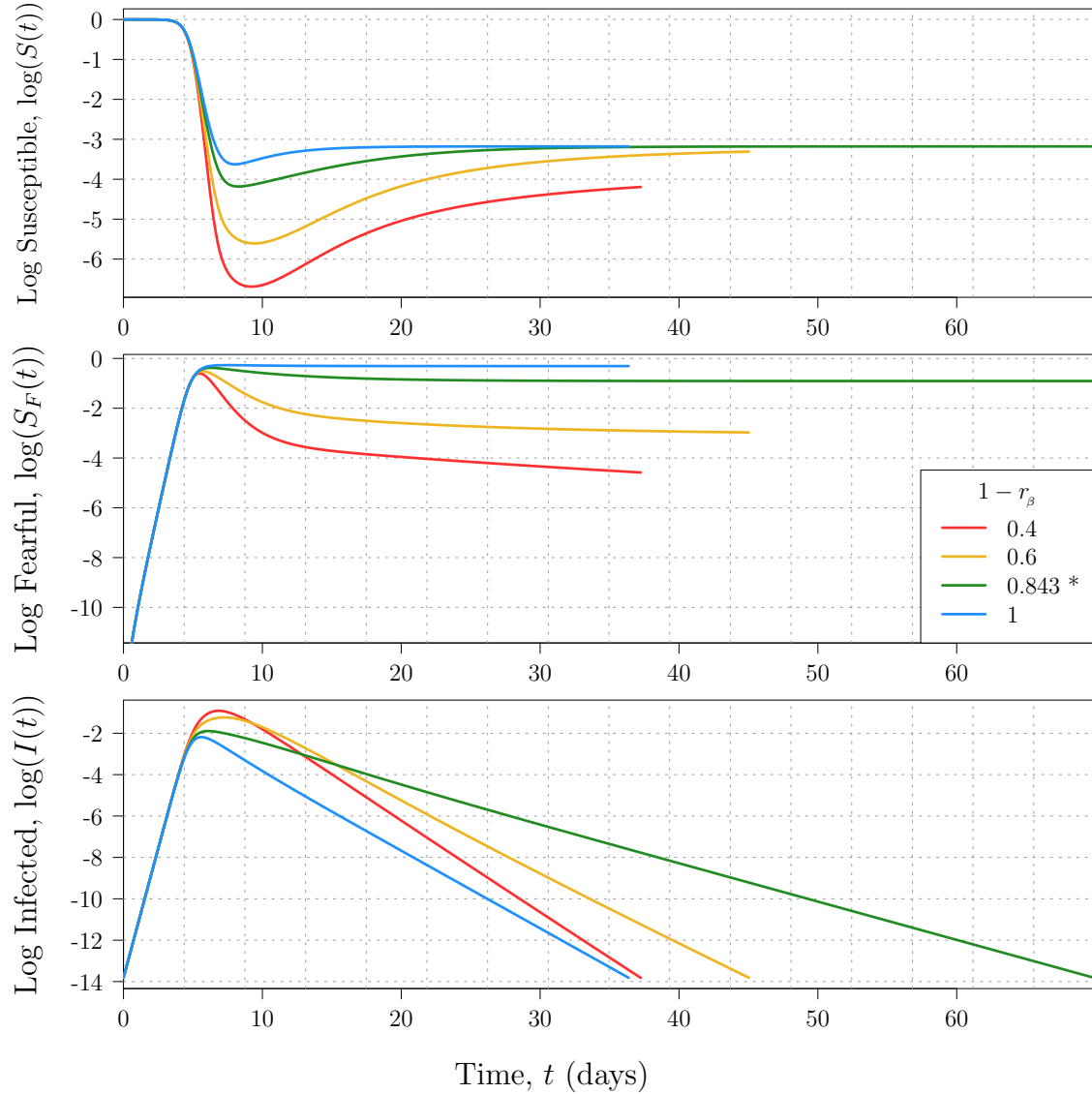


Figure 4.6: The proportion of susceptibles, $S(t)$, fearful susceptibles $S_F(t)$, and infected individuals $I(t)$ over time for values of the effectiveness of fear, $1 - r_\beta$, at and around the critical value that provokes the maximal time to extinction in the bSIR-PF model. The value of $1 - r_\beta$ exactly at the critical value is marked with an asterisk in the legend. State variables are plotted on a logarithmic scale to more clearly display any oscillatory behaviour. Parameter values for this plot correspond to those used in figure 4.5.

4.2.2 Final Size

Figure 4.7 shows the final size as a function of the effectiveness of fear in the bSIR-PF model.

When fear transmits quickly relative to infection (row 1 of figure 4.7), or both transmissions occur with equal speed (row 2 of the same figure), the relationship between effectiveness of fear and final size is monotonically decreasing. Recall from the bSIR-P case that in the region where final size decreases monotonically, it is because frightened individuals are contributing steadily to the first (and only) epidemic. The larger the proportion of frightened susceptibles, the less of a delay between the main epidemic and their contribution to the proportion of infected people via their infection. The shortening of this delay is due to the fact that if the prevalence of the disease is larger, the force of infection is stronger. When this delay is increased (if the proportion of frightened susceptibles is smaller), that is when the relationship between effectiveness of fear and final size becomes non-monotonic (see section 4.1.2).

In the bSIR-PF model, fear self-reinforces, leading to overall higher levels of fear, decreasing the delay between the main epidemic and the contribution from frightened susceptibles, allowing for a monotonically decreasing relationship between final size and effectiveness of fear in the cases where fear transmission is either faster than or equal to the rate of infection.

In the case where fear is slow relative to infection (row 3 of figure 4.5), a similar pattern is observed as in the same case with the bSIR-P model, except that there is a sharp spike in final size with the bSIR-PF model near the transition between one and two waves of infection instead of a steady increase from that point as in the bSIR-P model. The sharp spike is a result of the self-reinforcement of fear, which leads to a larger store of susceptibles that can contribute to a larger second epidemic, increasing the final size dramatically.

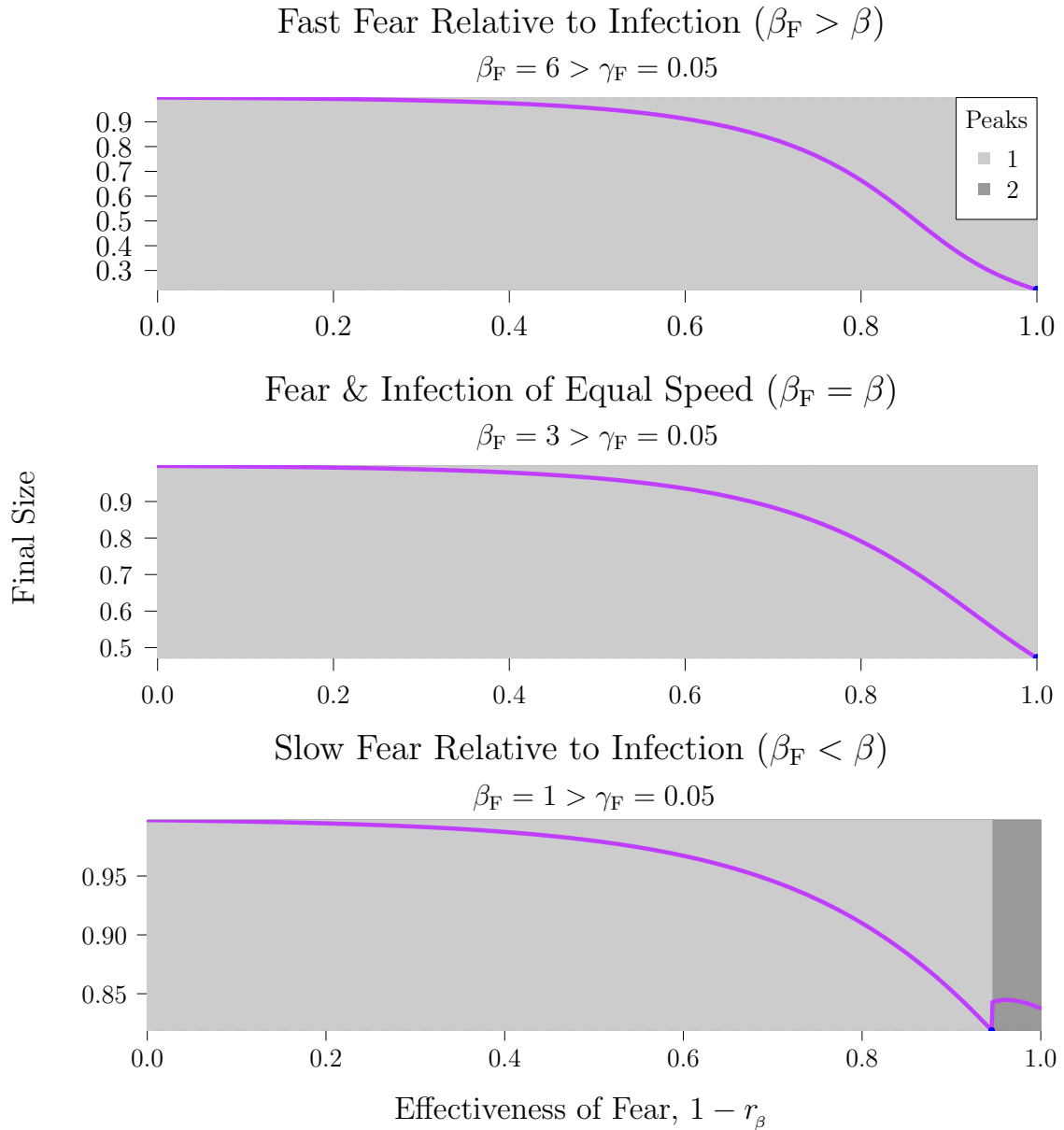


Figure 4.7: Final size as a function of the effectiveness of fear ($1 - r_\beta$) for three different parameter sets in the bSIR-PF model. This figure is analogous to figure 4.3 for the bSIR-P model.

4.2.3 Peak Prevalences

The peak prevalence of each epidemic is plotted as a function of the effectiveness of fear in figure 4.8.

Again, the peak prevalence decreases monotonically as the effectiveness of fear increases, and a second epidemic only appears in the case where the transmission of fear is slow relative to infection (but only for very effective fear). It is more difficult to provoke a second epidemic in this model where fear self-reinforces, as frightened individuals contribute more readily to the main epidemic.

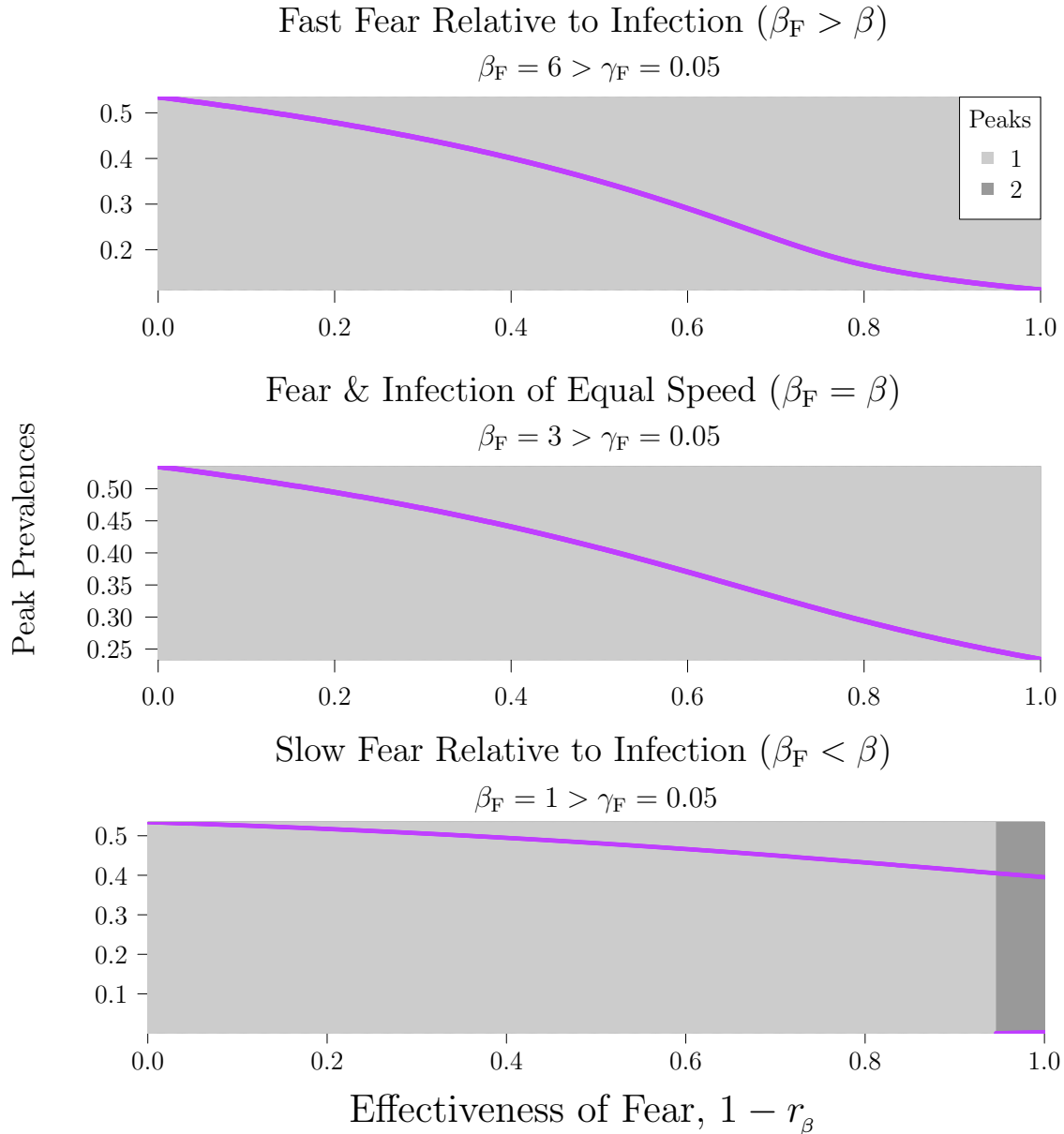


Figure 4.8: Peak prevalence of each epidemic as a function of the effectiveness of fear ($1 - r_\beta$) for three different parameter sets in the bSIR-PF model. This figure is analogous to figure 4.4 for the bSIR-P model.

4.3 Discussion

Based on the above analysis, it is clear that fear can lead to a variety of interesting and potentially important effects on the outbreak length, final size, and peak prevalence. Although the details of the effect may be different for each metric, it seems that there is a common thread running through all of them. Namely, that the relative rates of the transmission of fear and infection are important because the timing and length of the contribution of frightened individuals to infection can change epidemic outcomes dramatically. If the delay between the main epidemic (driven by the infection of fully susceptible individuals) and the infection of frightened individuals is short, these fearful susceptibles contribute to the main epidemic, and the effect on the three public health metrics under consideration align with expectations. If the delay is long, fearful susceptibles do not contribute to the main epidemic significantly, and the results again align with expectations. However, if the delay is intermediate, time to extinction may be prolonged significantly, the final size may be minimized, and a second epidemic may occur. Thus, it is important to understand how delayed the contribution of fearful individuals to the infection will be to properly predict the effect of fear on epidemiological metrics of importance in public health.

In the model with both prevalence- and fear-based fear, fear self-reinforces, which leads to overall higher levels of fear than in the case of only prevalence-based fear. It becomes more difficult to provoke a second wave of infection as fearful individuals contribute instead to the main epidemic. In other words, the delay between the main epidemic driven by fully susceptible individuals and the infection of fearful individuals is generally shortened in the model with fear-based spread of fear compared to the model with solely prevalence-based fear.

Chapter 5

Conclusion

In this thesis, I have incorporated adaptive human behaviour due to fear of an infectious disease into a simple epidemic model and analyzed this class of models in a variety of ways. Although the implementation of fear into the model is very simple, the resultant dynamics are rather rich.

I performed a standard dynamical analysis on the systems of ODEs associated with the behavioural models (chapter 2) and analyzed these models more rigourously than previously [19]. I attempted to understand the complex dynamics of these models further by trying to approximate one behavioural model in two different ways (chapter 3). I considered the effects of fear in these models on important public health metrics (chapter 4) in a much more thorough and systematic way than previously [19]. Moreover, I studied the effects of fear on two important public health metrics (the epidemic length and peak prevalence) that had not been previously addressed.

In performing this study, it has become clear that individual-level behaviour (such as the adoption of protective behaviours due to fear of the disease) can complicate population dynamics significantly, even when individual behaviour is fully deterministic. Furthermore, it is not always the case that the most efficient protective behaviour leads to the most favourable public health outcomes; sometimes an intermediate level of diligence, although potentially undesirable for the individual, is optimal for the population. For instance, in some cases where fear transmission is faster than the recovery from fear, the final size reaches a minimum when fear is intermediately effective. The conflict between individual self-interest and what is best for the population has been studied previously in similar systems [30–32].

All of the work in this thesis has been fully deterministic; a valuable direction for future work would be to consider a stochastic approach, which is more appropriate for biological populations where individuals are discrete and no event happens with full certainty [33–35]. For instance, instead of calculating the deterministic value of public health metrics like the outbreak length, final size, or peak prevalence, one could calculate a distribution of these quantities for a large number of stochastic simulations. These distributions could be used to attach some level of confidence in the predictions of these public health metrics. Moreover, statistical relationships among these metrics could also be explored.

Bibliography

- [1] Edelstein-Keshet L. *Mathematical Models in Biology*. Classics in Applied Mathematics. Society for Industrial and Applied Mathematics; 1988. Available from: <https://books.google.ca/books?id=uABYP1hnsf0C>.
- [2] Otto SP, Day T. *A Biologist's Guide to Mathematical Modeling in Ecology and Evolution*. Princeton University Press; 2011. Available from: <https://books.google.ca/books?id=vnNhcE9UwYcC>.
- [3] Ellner SP, Guckenheimer J. *Dynamic Models in Biology*. Princeton University Press; 2006. Available from: <https://books.google.ca/books?id=Wde1-JY04hIC>.
- [4] Anderson RM, May RM. *Infectious diseases of humans*. vol. 1. Oxford University Press; 1991.
- [5] Hethcote HW. *The mathematics of infectious diseases*. SIAM Review. 2000;42(4):599–653.
- [6] Keeling M, Rohani P. *Modeling Infectious Diseases in Humans and Animals*. Princeton University Press; 2011.
- [7] Murray JD. *Mathematical Biology*. 2nd ed. Springer-Verlag Inc.; 1993.
- [8] Brauer F, Castillo-Chavez C. *Mathematical models in population biology and epidemiology*. vol. 40 of Texts in Applied Mathematics. Springer-Verlag; 2001.
- [9] Ferguson N. *Capturing human behaviour*. Nature. 2007 April;446(7137):733. Available from: <http://dx.doi.org/10.1038/446733a>.
- [10] Epstein JM, Parker J, Cummings D, Hammond RA. *Coupled contagion dynamics of fear and disease: mathematical and computational explorations*. PLoS

- One. 2008 Jan;3(12):e3955. Available from: <http://dx.doi.org/10.1371/journal.pone.0003955>.
- [11] Funk S, Gilad E, Watkins C, Jansen VA. *The spread of awareness and its impact on epidemic outbreaks*. Proceedings of the National Academy of Sciences. 2009;106(16):6872–6877.
 - [12] Funk S, Salathé M, Jansen V. *Modelling the influence of human behaviour on the spread of infectious diseases: a review*. Journal of the Royal Society Interface. 2010;7:1247–1256. Available from: <http://dx.doi.org/10.1098/rsif.2010.0142>.
 - [13] Bootsma MC, Ferguson NM. *The effect of public health measures on the 1918 influenza pandemic in US cities*. Proceedings of the National Academy of Sciences. 2007;104(18):7588–7593.
 - [14] Caley P, Philp DJ, McCracken K. *Quantifying social distancing arising from pandemic influenza*. Journal of the Royal Society Interface. 2008;5(23):631–639.
 - [15] He D, Dushoff J, Day T, Ma J, Earn DJD. *Mechanistic modelling of the three waves of the 1918 influenza pandemic*. Theoretical Ecology. 2011 March;4(2):283–288. Available from: <http://dx.doi.org/10.1007/s12080-011-0123-3>.
 - [16] He D, Dushoff J, Day T, Ma J, Earn DJD. *Inferring the causes of the three waves of the 1918 influenza pandemic in England and Wales*. Proceedings of the Royal Society of London B. 2013 Sep;280(1766):20131345. Available from: <http://dx.doi.org/10.1098/rspb.2013.1345>.
 - [17] Liu R, Wu J, Zhu H. *Media/psychological impact on multiple outbreaks of emerging infectious diseases*. Computational and Mathematical Methods in Medicine. 2007;8(3):153–164.
 - [18] Poletti P, Caprile B, Ajelli M, Pugliese A, Merler S. *Spontaneous behavioural changes in response to epidemics*. Journal of Theoretical Biology. 2009 September;260(1):31–40. Available from: <http://dx.doi.org/10.1016/j.jtbi.2009.04.029>.
 - [19] Perra N, Balcan D, Gonçalves B, Vespignani A. *Towards a characterization of behavior-disease models*. PLoS One. 2011;6(8):e23084. Available from: <http://www.ncbi.nlm.nih.gov/pmc/articles/PMC3149628/>&tool=pmcentrez&rendertype=abstract.

- [20] Earn DJD. *Mathematics 4MB3/6MB3 Mathematical Biology*; 2014. <http://lalashan.mcmaster.ca/theobio/4MB3/index.php/Lectures>.
- [21] Bolker B. *fitsir: SIR fitting tools*; R package version 0.0-1. Available from: <https://github.com/bbolker/fitsir>.
- [22] Keeling MJ, Grenfell B. *Disease extinction and community size: modeling the persistence of measles*. Science. 1997;275(5296):65–67.
- [23] Nåsell I. *On the time to extinction in recurrent epidemics*. Journal of the Royal Statistical Society Series B-Statistical Methodology. 1999;61:309–330.
- [24] Hagenaars T, Donnelly C, Ferguson N. *Spatial heterogeneity and the persistence of infectious diseases*. Journal of Theoretical Biology. 2004;229(3):349–359.
- [25] Grenfell BT, Pybus OG, Gog JR, Wood JL, Daly JM, Mumford JA, et al. *Unifying the epidemiological and evolutionary dynamics of pathogens*. Science. 2004;303(5656):327–332.
- [26] Kermack WO, McKendrick AG. *A contribution to the mathematical theory of epidemics*. Proceedings of the Royal Society of London A. 1927;115:700–721.
- [27] Ball F, Nåsell I. *The shape of the size distribution of an epidemic in a finite population*. Mathematical Biosciences. 1994;123(2):167–181.
- [28] Keeling MJ. *The effects of local spatial structure on epidemiological invasions*. Proceedings of the Royal Society of London B. 1999;266(1421):859–867.
- [29] Ma J, Earn DJD. *Generality of the final size formula for an epidemic of a newly invading infectious disease*. Bulletin of Mathematical Biology. 2006;68(3):679–702. Available from: <http://dx.doi.org/10.1007/s11538-005-9047-7>.
- [30] Bauch CT, Galvani AP, Earn DJD. *Group interest versus self-interest in smallpox vaccination policy*. Proceedings of the National Academy of Sciences. 2003;100(18):10564–10567.
- [31] Bauch CT, Earn DJD. *Vaccination and the theory of games*. Proceedings of the National Academy of Sciences. 2004;101(36):13391–13394.
- [32] Molina C, Earn DJD. *Game theory of pre-emptive vaccination before bioterrorism or accidental release of smallpox*. Journal of The Royal Society Interface. 2015;12(107):20141387.

- [33] Bartlett MS. *An introduction to stochastic processes, with special reference to methods and applications.* CUP Archive; 1978.
- [34] Bailey NT. *The elements of stochastic processes with applications to the natural sciences.* vol. 25. John Wiley & Sons; 1990.
- [35] Allen LJ. *An introduction to stochastic processes with applications to biology.* CRC Press; 2010.
- [36] Hirsch MW, Smale S, Devaney RL. *Differential equations, dynamical systems, and an introduction to chaos.* 3rd ed. Academic Press; 2013.
- [37] Soetaert K, Petzoldt T, Setzer RW. *Solving Differential Equations in R: Package deSolve.* Journal of Statistical Software. 2010;33(9):1–25. Available from: <http://www.jstatsoft.org/v33/i09>.
- [38] Papst I. *Improving Performance of Numerical Integration in R (CSE 701 - Final Project);* 2014. Unpublished.
- [39] Soetaert K, Petzoldt T, Setzer RW. *R Package deSolve, Writing Code in Compiled Languages;.* Available from: <http://cran.r-project.org/web/packages/deSolve/vignettes/compiledCode.pdf>.

Appendix A

Proof of Lemma 1

We want to show that solutions to our system of ODEs (2.11) with biologically well-defined initial conditions (2.14) remain biologically well-defined as time evolves (*i.e.*, that (2.15) holds).

Since none of the equations depend on R , we can reduce our state-space to $(S, S_F, I) \in \mathbb{R}^3$. Thus, to prove the theorem, we can do so by showing that the domain

$$\Delta := \{(S, S_F, I) \in \mathbb{R}^3 \mid (S \geq 0), (S_F \geq 0), (I \geq 0), (0 \leq S + S_F + I \leq 1)\} \quad (\text{A.1})$$

(a triangle-based pyramid in the first octant) is positively invariant with respect to time.

Firstly, we want to establish that the solution curves to the initial value problem given by (2.11) and $(S(0), S_F(0), I(0)) \in \Delta$ (*i.e.*, the trajectories) are continuous. To do so, we will make use of the following theorem:

Theorem 2 (Continuous Dependence on Initial Conditions [36]). *Let $\phi(t, X)$ be the flow of the system $X' = F(X)$ where F is C^1 . Then ϕ is a continuous function of X .*

Letting $X = (S, S_F, I)$, and writing the system of ODEs in vector form as $X' = F(X)$, we see that F is a C^1 function and so by theorem 2, solution trajectories (flows) are continuous.

Since trajectories for the system are continuous, it's sufficient to show that no

solution beginning in Δ can escape its boundary

$$\partial\Delta = \{(S, S_F, I) \in \mathbb{R}^3 \mid \textcircled{1}, \textcircled{2}, \textcircled{3}, \textcircled{4}\}, \quad (\text{A.2})$$

where

$$\textcircled{1} = (S = 0), (S_F \geq 0), (I \geq 0), (S_F + I \leq 1), \quad (\text{A.3a})$$

$$\textcircled{2} = (S_F = 0), (S \geq 0), (I \geq 0), (S + I \leq 1), \quad (\text{A.3b})$$

$$\textcircled{3} = (I = 0), (S \geq 0), (S_F \geq 0), (S + S_F \leq 1), \quad (\text{A.3c})$$

$$\textcircled{4} = (S \geq 0), (S_F \geq 0), (I \geq 0), (S + S_F + I = 1). \quad (\text{A.3d})$$

Region $\textcircled{1} \subset \partial\Delta$:

First off, consider planar subset $\textcircled{1} \subset \partial\Delta$. In this region, $S = 0$, and so

$$\frac{dS}{dt} = \gamma_F S_F (1 - I). \quad (\text{A.4})$$

We assume that $S_F \geq 0$ and $I \geq 0$ in this region, that all parameters are positive, and that $S_F + I \leq 1$ so I is at most equal to 1 and $1 - I \geq 0$. Thus, (A.4) is non-negative in this region, which means that S can only increase from zero into the interior of Δ .

Now we just need to show that the two other state variables, S_F and I , cannot exceed their bounds in $\textcircled{1}$. The bounds on S_F and I in this region are given by the boundary of $\textcircled{1}$, a subset of the $S_F I$ -plane,

$$\partial\textcircled{1} = \{(S_F, I) \in \mathbb{R}^2 \mid (S_F = 0), (I = 0), (S_F + I = 1)\}. \quad (\text{A.5})$$

Since $S = 0$,

$$\frac{dS_F}{dt} = -r_\beta \beta S_F I - \gamma_F S_F (1 - I), \quad (\text{A.6})$$

$$\frac{dI}{dt} = (r_\beta \beta S_F - \gamma) I. \quad (\text{A.7})$$

If $I(0) = 0$, $dI/dt = 0$ and so $I(t) \equiv 0$ and cannot decrease below 0 to escape Δ in this part of $\partial\Delta$, while (A.6) reduces to $dS_F/dt = -\gamma_F S_F$, which means that S_F decreases down this I -nullcline from its initial value (which is assumed to be $0 \leq S_F(0) \leq 1$). Moreover, S_F cannot decrease past 0 since if $S_F(\tau) = 0$ for some time $t = \tau$, $dS_F/dt(\tau) = 0$ and so $S_F(t) = 0 \forall t \geq \tau$. Thus, a trajectory beginning in

Δ cannot escape along the line $I = 0$.

Symmetrically, if $S_F(0) = 0$, then $dS_F/dt = 0$, and (A.7) reduces to $dI/dt = -\gamma I$, so the same argument as above holds.

Lastly, note that everywhere in Δ ,

$$\frac{d(S + S_F + I)}{dt} = -\gamma I \leq 0, \quad (\text{A.8})$$

so $S + S_F + I$ is always non-increasing, which means that, since $S = 0$ in ①, $S_F(t) + I(t) \leq S_F(0) + I(0) = 1$.

Therefore, trajectories beginning in Δ cannot escape this domain through ① $\subset \partial\Delta$.

Region ② $\subset \partial\Delta$:

The approach here is identical as for region ①.

Since $S_F = 0$, then

$$\frac{dS_F}{dt} = \beta_F SI \geq 0. \quad (\text{A.9})$$

In other words, S_F can only increase from zero back into the interior of Δ .

Now we consider the boundary of region ②,

$$\partial\textcircled{2} = \{(S, I) \in \mathbb{R}^2 \mid (S = 0), (I = 0), (S + I = 1)\}. \quad (\text{A.10})$$

Since $S_F = 0$,

$$\frac{dS}{dt} = -(\beta_F + \beta)SI, \quad (\text{A.11})$$

$$\frac{dI}{dt} = (\beta S - \gamma)I. \quad (\text{A.12})$$

If $I(0) = 0$, both dS/dt and dI/dt are zero, so $I(t) \equiv 0$ and $S(t) = S(0)$ so $0 \leq S(t) \leq 1 \forall t > 0$.

If $S(0) = 0$, $dS/dt = 0$, so $S(t) \equiv 0$, while $dI/dt = -\gamma I \leq 0$, so $0 \leq I(0) \leq 1$ implies that $0 \leq I(t) \leq 1 \forall t \geq 0$.

Lastly, again by (A.8), if $S(0) + I(0) = 1$, $S(t) + I(t) \leq 1 \forall t \geq 0$.

Therefore, trajectories with initial conditions (2.14) cannot escape out of the

domain Δ via $\textcircled{2} \subset \Delta$.

Region $\textcircled{4} \subset \Delta$:

By (A.8), we have that $S + S_F + I$ is non-increasing everywhere in Δ , and so $S(t) + S_F(t) + I(t) \leq S(0) + S_F(0) + I(0) = 1 \forall t \geq 0$. In other words, trajectories will be pushed into the interior of Δ from $\textcircled{4}$.

Region $\textcircled{3} \subset \Delta$:

Again, the approach here is identical to the one used for previously discussed regions of $\partial\Delta$.

Since $I = 0$, $dI/dt = 0$, and so the trajectory stops moving in the I -direction as soon as $I = 0$. Thus I cannot decrease past zero and become negative.

Now we consider the boundary of region $\textcircled{3}$,

$$\partial\textcircled{3} = \{(S, S_F) \in \mathbb{R}^2 \mid (S = 0), (S_F = 0), (S + S_F = 1)\}. \quad (\text{A.13})$$

Since $I = 0$,

$$\frac{dS}{dt} = \gamma_F S_F, \quad (\text{A.14})$$

$$\frac{dS_F}{dt} = -\gamma_F S_F. \quad (\text{A.15})$$

Note that $d(S + S_F)/dt = 0$, so $S(t) + S_F(t) = S(\tau) + S_F(\tau)$, where τ is the time at which I is first zero. Since we have already shown that trajectories cannot escape Δ everywhere except $\Delta \setminus \text{int}(\textcircled{3})$, we know that $0 \leq S(\tau) + S_F(\tau) \leq 1$, and so $0 \leq S(t) \leq 1$ and $0 \leq S_F(t) \leq 1$.

Thus, we conclude that, for positive parameter values, if we choose initial conditions that satisfy (2.14), then (2.15) holds – that is trajectories are always biologically well-defined as time evolves.

Appendix B

Sample Code for SIR Fitting

B.1 Preliminaries

The following codes were written and run on a Macintosh computer with:

1. Mac OS X version 10.10.4
2.  version 3.1.2 (2014-10-31) – “Pumpkin Helmet”

All scripts are written in  unless otherwise stated.

B.2 Numerically Solving the bSIR Equations

To fit an SIR model to bSIR data, we must first generate bSIR data to fit. We do so by numerically solving the bSIR differential equations with set initial conditions and parameters. We accomplish this using the `deSolve` package for  [37].

Generally, numerical integration using the `deSolve` package is relatively fast if a small number of integrations are performed. However, when fitting a model to data, many integrations may be necessary and so using a compiled gradient could significantly speed up the process [38]. To implement a compiled gradient with our integrator, we use the `compiledCode` package for  [39].

B.2.1 Compiled Gradient

We use the following compiled gradient coded in C (along with the  script from the subsequent section) to numerically solve the system of ODEs:

```

/* bSIR_PF.c */
/* Author: Irena Papst */

/* The bSIR gradient in C for use with R */
/* State variables are in units of proportions of
individuals
and "healthy" people are assumed to be all those who
are not infected */
/* Compile on the command line with
R CMD SHLIB bSIR_PF.c */

#include <R.h> // include R library

/* define parameter array globally */

static double parms[6];

/* order of params in array must match the order in
which they are passed from R to the DLL */

#define beta parms[0]
#define beta_F parms[1]
#define gamma_F parms[2]
#define r_beta parms[3]
#define gamma parms[4]
#define rbetaF parms[5]

/* define initializer for parms passed from R */

void initmod(void (*odeparms)(int *, double *))
{
    int num=6;
    odeparms(&num, parms);
}

```

```

}

/* define derivatives function */

void derivs (int *neq, // points to the number of
equations
            double *t, // points to time
            double *vars, // points to a double
precision array of length neq that
containing the current value of the
state variables
            double *varsdot, // points to an array
that contains the calculated
derivatives
            double *varsout, // points to a vector
whose first nout elements are other
output variables (different from the
state variables), followed by the
double vals passed by parameters rpar
when calling the integrator
            int *ip // points to an integer vector
with length at least 3
// first element contains the number of output values (
should be equal to or larger than nout)
// second element contains the length of yout
// third element contains the length of op
// next are integer values, as passed by the parameter
ipar when calling the integrator
)
{
    if (ip[0] <1) error("nout should be at least 1.");
    // check whether nout is at least 1
    varsdot[0] = - beta*vars[2]*vars[0] - beta_F*vars
[0]*vars[2] - rbetaF*beta_F*vars[0]*vars[1] +
gamma_F*vars[1]*(1-vars[2]); // equation for S
}

```

```

varsdot[1] = - r_beta*beta*vars[1]*vars[2] + beta_F
            *vars[0]*vars[2] + rbetaF*beta_F*vars[0]*vars[1]
            - gamma_F*vars[1]*(1-vars[2]); // equation for
            S_F
varsdot[2] = - gamma*vars[2] + beta*vars[0]*vars[2]
            + r_beta*beta*vars[1]*vars[2]; // equation for
            I
varsdot[3] = beta*vars[0]*vars[2] + r_beta*beta*
            vars[1]*vars[2]; // equation for Z, the
            cumulative case count

varsout[0] = 1 - vars[0] - vars[1] - vars[2]; //
            calculate R(t)
varsout[1] = varsdot[2]; // export dI/dt (to
            calculate number of peaks)
}

```

B.2.2 Numerical Integration Script

```

## Load package to numerically solve ODEs
library("deSolve")

## Define a function to numerically solve the bSIR
## equations
## with a C gradient for speed
bSIRsolve <- function(tmax, # max integration time, in
days
  S0, S_F0, I0, # initial conditions
                in proportions of the population
  beta, beta_F, gamma_F, r_beta, gamma
                , N, # parameters
  rbetaF=0 # rbetaF value for prev-
                and fear-based spread (if 0, then
                there is just prev-based fear)
) {

```

```

## Set integration parameters
stepsize <- 1/24

# Solve the odes numerically using the previously
# defined R gradient
Z0 <- IO # set initial cumulative case count equal to
# the initial number of infecteds

## Load DLL
dyn.load("~/Dropbox/bSIR/scripts/bSIR_PF.so")
## Solve ODE
soln <- ode(y=c(S=S0,S_F=S_F0,I=IO,Z=Z0),
              times=seq(0, tmax, by=stepsize),
              func="derivs",
              parms=c(beta=beta, beta_F=beta_F, gamma_F=
                      gamma_F, r_beta=r_beta, gamma=gamma,
                      rbetaF=rbetaF),
              dllname = "bSIR_PF",
              initfunc = "initmod",
              nout = 2, outnames = c("R", "dI"))
soln <- as.data.frame(soln)

## If prevalence falls below one individual
## stop returning data
ind <- which(soln$I<1/N)
if (length(ind)>0){
  soln <- soln[1:min(ind),]
}

return(soln)
}

```

B.2.3 Generating bSIR Data

We then generate the bSIR data using the following script:

```

## Set up parms.df (parameter dataframe)
R0.vec <- c(rep(2,7)) # basic reproduction number

```

```

beta_F.vec <- c(0.25, 0, 1, 2.5, 5, 3, 3) # transmission
      of fear
gamma_F.vec <- c(rep(0.5,5), 0.1, 0.05) # recovery rate
      from fear
r_beta.vec <- c(rep(0.5,5), 0.1, 0.1) # constant of
      proportionality
# between transmission rate for susceptibles and fearful
      susceptibles
gamma.vec <- c(rep(0.1,6), 0.5) # recovery rate from the
      disease
N.vec <- c(rep(1e6,7)) # population size
# transmission rate of the disease from the S compartment
# and the S_F compartment

## Define transmission term
beta.vec <- R0.vec*gamma.vec

## Set initial conditions (state variables are in numbers
      of individuals)
I0.vec <- rep(1, length(R0.vec))
S0.vec <- N.vec-I0.vec
S_F0.vec <- rep(0, length(R0.vec)) # no one is initially
      fearful

## Set max integration time
tmax <- 300

## Set up parameter array
parm.df <- data.frame(R0=R0.vec,
                       beta=beta.vec,
                       beta_F=beta_F.vec,
                       gamma_F=gamma_F.vec,
                       r_beta=r_beta.vec,
                       gamma=gamma.vec,
                       N=N.vec,
                       S0=S0.vec,
                       S_F0=S_F0.vec,
                       I0=I0.vec)

```

```

for(i in 1:7){
  parmsrow <- i

  ## Set parameters
  R0 <- parm.df$R0[parmsrow]
  beta <- parm.df$beta[parmsrow]
  beta_F <- parm.df$beta_F[parmsrow]
  gamma_F <- parm.df$gamma_F[parmsrow]
  r_beta <- parm.df$r_beta[parmsrow]
  gamma <- parm.df$gamma[parmsrow]
  N <- parm.df$N[parmsrow]
  S0 <- parm.df$S0[parmsrow]
  S_F0 <- parm.df$S_F0[parmsrow]
  IO <- parm.df$IO[parmsrow]

  ## Generate data
  bSIRdata <- bSIRsolve(tmax=tmax,
                         SO=S0, S_F0=S_F0, IO=IO,
                         beta=beta, beta_F=beta_F, gamma_F=
                           gamma_F,
                         r_beta=r_beta, gamma=gamma)

  ## Relabel the data with a fitsir-friendly format
  bSIRdata <- data.frame(tvec=bSIRdata$time, count=
    bSIRdata$I)

  ## Store parameter set used for these data
  parms <- parm.df[parmsrow,]

  ## Save objects to .Rdata file
  save(list=c("bSIRdata", "parms"),
        file=paste0("data/bSIR-parmsrow", parmsrow, ".Rdata"))
}

```

B.3 Fitting an SIR Model to bSIR Data

Lastly, we fit an SIR model to bSIR prevalence data and plot the fit with the following script:

```

fitsirplot <- function(paramset=2,
                        bSIRlwd=12,
                        plotcex=0.75,
                        margins=c(2.5,2.5,0.1,0.1)+0.1
) {

  ## Load pre-generated bSIR data
  load(paste0("data/bSIR-parmsrow", " .Rdata"))

  ## Source files
  library("fitsir")
  library("bbmle")

  ## Rename parameters for cleaner code
  R0 <- parms$R0
  beta <- parms$beta
  beta_F <- parms$beta_F
  gamma_F <- parms$gamma_F
  r_beta <- parms$r_beta
  gamma <- parms$gamma
  N <- parms$N
  S0 <- parms$S0
  S_F0 <- parms$S_F0
  I0 <- parms$I0

  ## Fit calculation
  m1 <- fitsir(data=bSIRdata, start=startfun(log.beta=log(
    beta),
    log.gamma=log(
      gamma),
    log.N=log(N),

```

```

        logit.i=
          qlogis(I0/
N)))

## Simulate SIR with fitted parameters
SIRfitdata <- with(bSIRdata, SIR.detsim(tvec,trans.pars(
  coef(m1)))))

## Set plotting parameters
bSIRcol <- "#FF8000"
SIRcol <- "blue"
SIRlwd <- bSIRlwd/3

## Set up plotting region
#par(mar=c(5,5,1,8.25)+0.1)
par(mar=margins)

## Set mult factor to expand plot limits
limmult <- 1.05

## Set mult factor to position legend in margin
xlegmult <- 1.05
ylegmult <- 1.13

## Plot bSIR "data"
plot((count/N)^tvec, data=bSIRdata,
      type="l", xaxs="i",
      xlab="", ylab="",
      col=bSIRcol, lwd=bSIRlwd,
      ylim=c(0, max(count/N)),
      cex.axis=plotcex, cex.lab=plotcex, las=1)

## Add fitted SIR solution
lines(bSIRdata$tvec, SIRfitdata/N, col=SIRcol, lwd=
SIRlwd)

## Log-Likelihood
loglikelihood <- sprintf("%g", as.numeric(logLik(m1)))

```

```
legend(0.6*max(bSIRdata$tvec), 1.05*max(bSIRdata$count/N
),
      #xlegmult*max(bSIRdata$tvec), -0.03*max(bSIRdata$ 
      count),
      legend=loglikelihood,
      bty="n", title="\textbf{Log-Likelihood}", xpd=
      TRUE,
      cex=plotcex, title.adj=0)

## Parameter set label
parsetlab <- paste0("Parameter_Set", paramset-1)
title(main=paste0("$\\textbf{", parsetlab, "}$"), line
      =1)
}
```

Appendix C

Sample Code for Calculating Public Health Quantities

C.1 Preliminaries

We use the same system setup detailed in appendix [B.1](#).

C.2 Numerically Solving the bSIR Equations

In order to calculate any of the three public health metrics of interest in chapter [4](#), we must first numerically solve the bSIR differential equations with set initial conditions and parameters. We accomplish this using the same script as in appendix [B.2](#).

C.3 Number of Epidemic Peaks

To calculate the number of epidemic peaks, we want to know how many local maxima the prevalence curve has. A local maxima occurs when the derivative of a function goes through zero by going from positive to negative. Thus, to calculate the number of local maxima in a prevalence curve, we keep track of dI/dt at every time step during the numerical integration, and then apply the following custom  function to it:

```

## Function to calculate the number of waves in a
## prevalence time series from its derivative
numpeaks <- function(dI){
  ## Calculate the number of times the derivative is zero
  diff <- diff(sign(dI)) # calculate vector of element-
  ## wise differences
  zeros <- sum(diffs != 0) # count how many differences
  ## are non-zero (each difference that is != 0 is a zero
  ## of the derivative)

  ## Calculate the number of waves from the number of
  ## zeros
  if (zeros%%2==1){
    # for an odd number of zeros
    numpeaks <- (zeros+1)/2
  } else {
    # for an even number of zeros
    numpeaks <- zeros/2
  }

  return(numpeaks)
}

```

This function takes in dI/dt and first transforms each value into -1 , 0 , or 1 , if the number is negative, zero, or positive, respectively. Then the function takes the element-wise differences of this vector. If there is no change of sign, the difference will be zero. Thus, the function counts the number of differences that are non-zero; this action will catch *all* local extrema, including minima. However, since we know that, if an epidemic is going to take off, that is, if $\mathcal{R}_0 > 1$, then dI/dt will initially be positive. Moreover, since dI/dt is C^∞ , the first extremum will have to be a maximum. The next extremum will have to be a minimum by continuity, and the extrema will continue to alternate until the prevalence falls below one individual.

With this known pattern of extrema, we can calculate how many maxima there are based on whether the number of extrema (*i.e.*, the number of detected zeros in dI/dt) is even or odd. If the number of zeros, z is odd, then the number of zeros that are maxima, m , is given by $m = (z + 1)/2$. If the number of zeros is even, then the number of zeros that are maxima is given by $m = z/2$.

C.4 Epidemic Length

To calculate the epidemic length, we simply integrate the system of ODEs until prevalence falls below one individual, that is until $I(t) < 1/N$, and then take the first time at which this occurs.

```
## Set up function to calculate time to extinction
timeext <- function(R0=2,
                      gamma=0.5,
                      rbeta=0.1,
                      betaF=3,
                      gammaF=0.05,
                      N=1e6,
                      rbetaF=0
) {

# Set initial conditons
I0 <- 1/N
S0 <- 1-I0
S_F0 <- 0

## Calculate beta
beta <- R0*gamma

## Solve ODEs numerically once
tmax <- 300

soln <- bSIRsolve(tmax=tmax,
                    S0=S0, S_F0=S_F0, I0=I0,
                    beta=beta, beta_F=betaF, gamma_F=gammaF,
                    r_beta=rbeta, gamma=gamma, N=N, rbetaF=
                    rbetaF)

## Solve ODEs numerically until the number of infecteds is
## below one individual

while (soln$I[nrow(soln)]>1/N){
  tmax <- 1.5*tmax
```

```

soln <- bSIRsolve(tmax=tmax,
                     SO=SO, S_F0=S_F0, IO=IO,
                     beta=beta, beta_F=betaF, gamma_F=
                     gammaF,
                     r_beta=rbeta, gamma=gamma, N=N,
                     rbetaF=rbetaF)
}

# bSIR data is cut off at the point where soln$I dips
# below 1/N
# so the maximal output time is the time of extinction
timeext <- max(soln$time)

return(timeext)
}

```

C.5 Final Size

To calculate the final size, we keep track of the cumulative case count during our numerical integration of the system of ODEs. Just as with the calculation of epidemic length, we continue to integrate until prevalence falls below one individual, and then take the maximal cumulative case count, which is the final size.

```

## Set up function to calculate final size
finalsize <- function(R0=2,
                       gamma=0.5,
                       rbeta=0.1,
                       betaF=3,
                       gammaF=0.05,
                       N=1e6,
                       rbetaF=0
) {

# Set initial conditons
IO <- 1/N

```

```

S0 <- 1-IO
S_F0 <- 0

## Calculate beta
beta <- R0*gamma

## Solve odes numerically initially
tmax <- 300
soln <- bSIRsolve(tmax=tmax,
                     SO=S0, S_F0=S_F0, IO=IO,
                     beta=beta, beta_F=betaF, gamma_F=gammaF,
                     r_beta=rbeta, gamma=gamma, N=N, rbetaF=
                     rbetaF)

## Continue integrating until the epidemic burns out
while (soln$I[nrow(soln)]>1/N){
  tmax <- 1.5*tmax

  soln <- bSIRsolve(tmax=tmax,
                     SO=S0, S_F0=S_F0, IO=IO,
                     beta=beta, beta_F=betaF, gamma_F=gammaF,
                     r_beta=rbeta, gamma=gamma, N=N, rbetaF=
                     rbetaF)
}

## bSIRsolve output is cut off when I<1/N, so the last (maximal) value of Z is the final size
finalsize <- max(soln$Z)

return(finalsize)
}

```

C.6 Peak Prevalences

To calculate peak prevalence(s), we use a similar technique as for calculating the number of peaks (see section C.3) , except instead of counting the number of zeros

in dI/dt , we locate zeros that occur by going from positive to negative values and output the prevalence at these points in the numerical integration.

```
# Function to calculate the peak prevalence(s)
peakprev <- function(R0=2,
                      gamma=0.5,
                      rbeta=0.1,
                      betaF=3,
                      gammaF=0.05,
                      N=1e6,
                      rbetaF=0
) {

# Set initial conditons
IO <- 1/N
SO <- 1-IO
S_F0 <- 0

## Calculate beta
beta <- R0*gamma

## Solve ODEs numerically once
tmax <- 300

soln <- bSIRsolve(tmax=tmax,
                    SO=SO, S_F0=S_F0, IO=IO,
                    beta=beta, beta_F=betaF, gamma_F=gammaF,
                    r_beta=rbeta, gamma=gamma, N=N, rbetaF=
                    rbetaF)

## Solve ODEs numerically until the number of infecteds is
## below one individual

while (soln$I[nrow(soln)]>1/N){
  tmax <- 1.5*tmax

  soln <- bSIRsolve(tmax=tmax,
                     SO=SO, S_F0=S_F0, IO=IO,
```

```
        beta=beta , beta_F=betaF , gamma_F=
          gammaF ,
        r_beta=rbeta , gamma=gamma , N=N ,
        rbetaF=rbetaF)
}

## Now we need to find the peaks
## They will occur where dI/dt=0, but specifically when
## the derivative goes from positive to negative
## i.e. the difference between elements is negative

diffs <- diff(sign(soln$dI)) # calculate vector of element
  -wise differences
ind <- which(diffs<0) # find the indices for any negative
  differences
peakdata <- soln[ind,] # extract rows of ODE solution data
  where a peak occurs

return(peakdata)
}
```

Appendix D

Full Results from Chapter 4: The Effects of Fear on Public Health Quantities

D.1 The Behavioural SIR with Prevalence-Based Fear (bSIR-P)

D.1.1 Outbreak Length

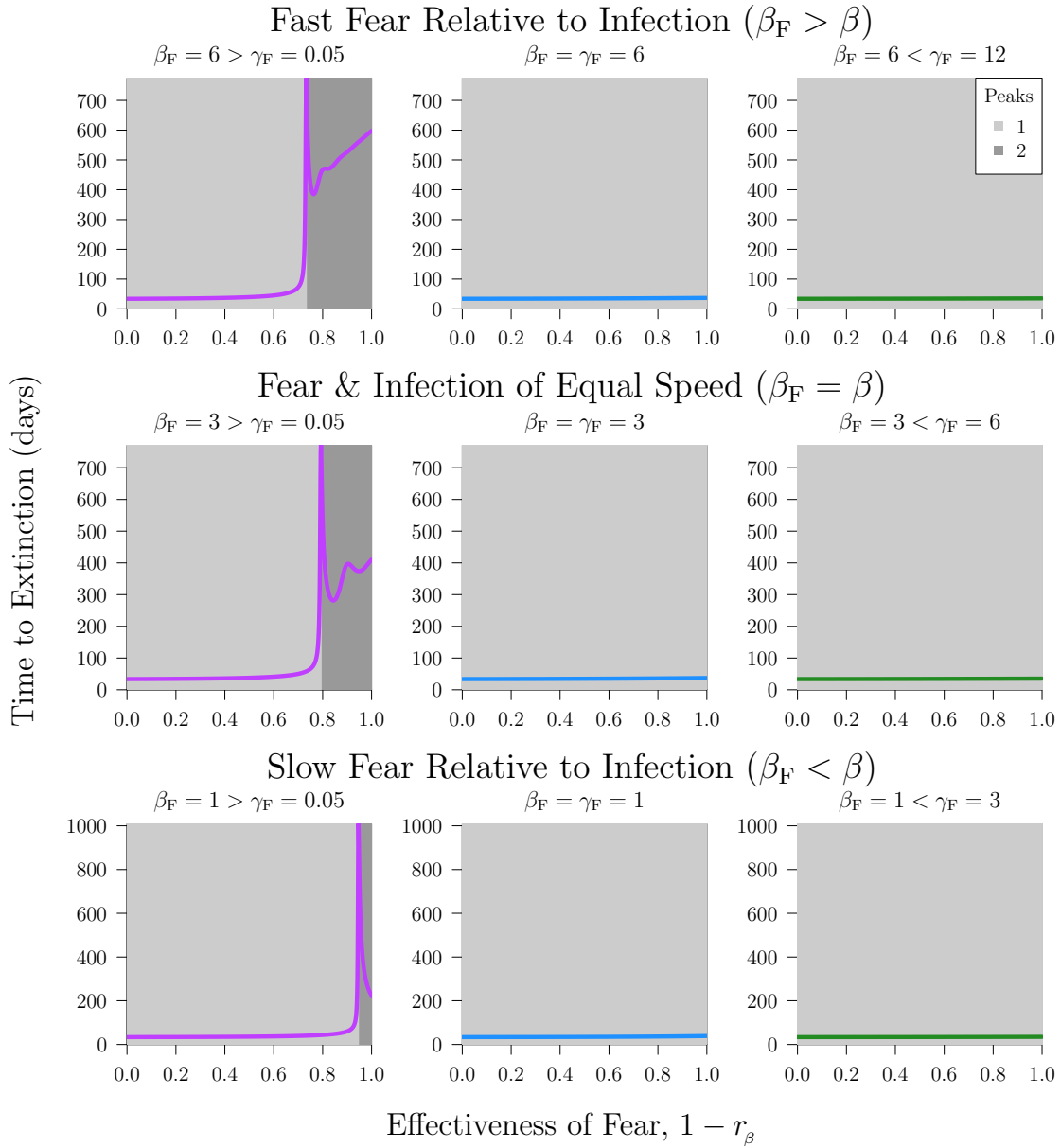


Figure D.1: Outbreak length (time to extinction) as a function of the effectiveness of fear ($1 - r_\beta$) for nine different parameter sets in the bSIR-P model. Infection parameters and the population size are fixed among the plots, with $\mathcal{R}_0 = 6$, $\gamma = 0.5 \text{ days}^{-1}$ (and thus $\beta = \mathcal{R}_0 \cdot \gamma = 3 \text{ days}^{-1}$), and $N = 10^6$ individuals. Fear parameters vary, as given in each plot title. Background shading denotes the number of peaks present in the prevalence curve for each fixed r_β value (and so for each fixed effectiveness of fear value).

D.1.2 Final Size

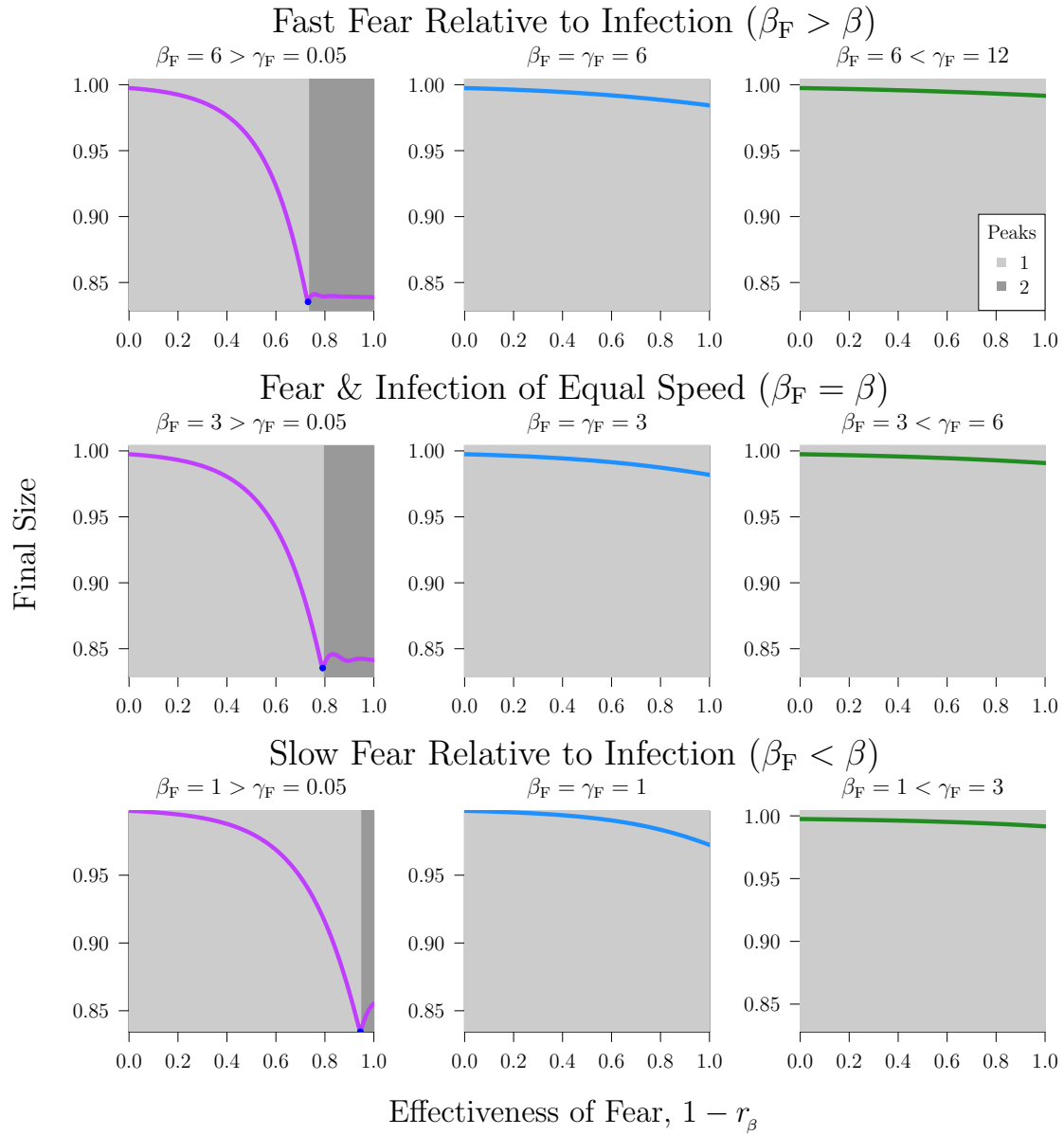


Figure D.2: Final size as a function of the effectiveness of fear ($1 - r_\beta$) for nine different parameter sets in the bSIR-P model. Parameter values are the same as in figure D.1. The minimum final size is denoted by a blue point.

D.1.3 Peak Prevalences

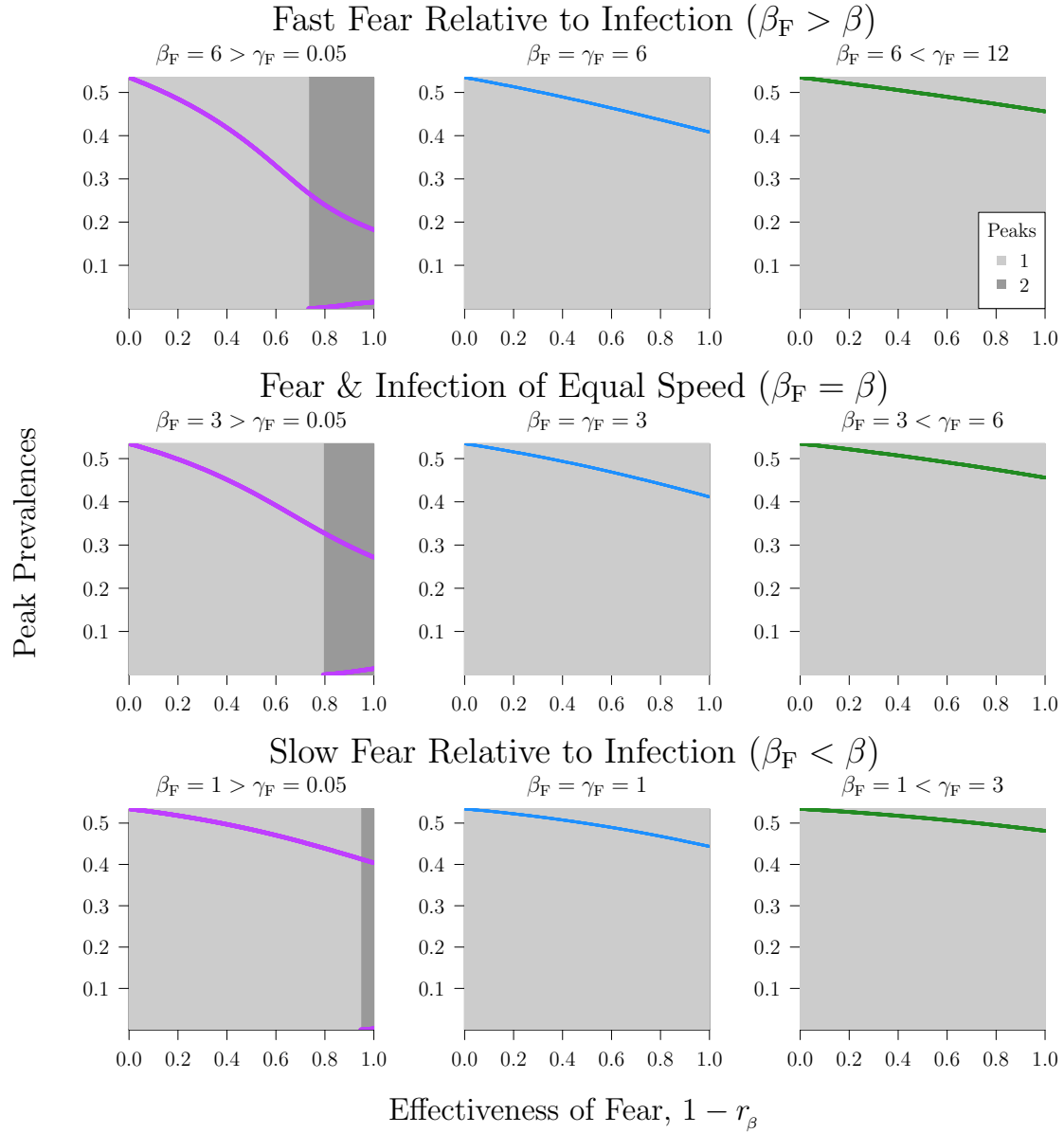


Figure D.3: The peak prevalence of each epidemic as a function of the effectiveness of fear ($1 - r_\beta$) for nine different parameter sets in the bSIR-P model. Parameter values are the same as in figure 4.1.

D.2 The Behavioural SIR with Prevalence- and Fear-Based Fear (bSIR-PF)

D.2.1 Outbreak Length

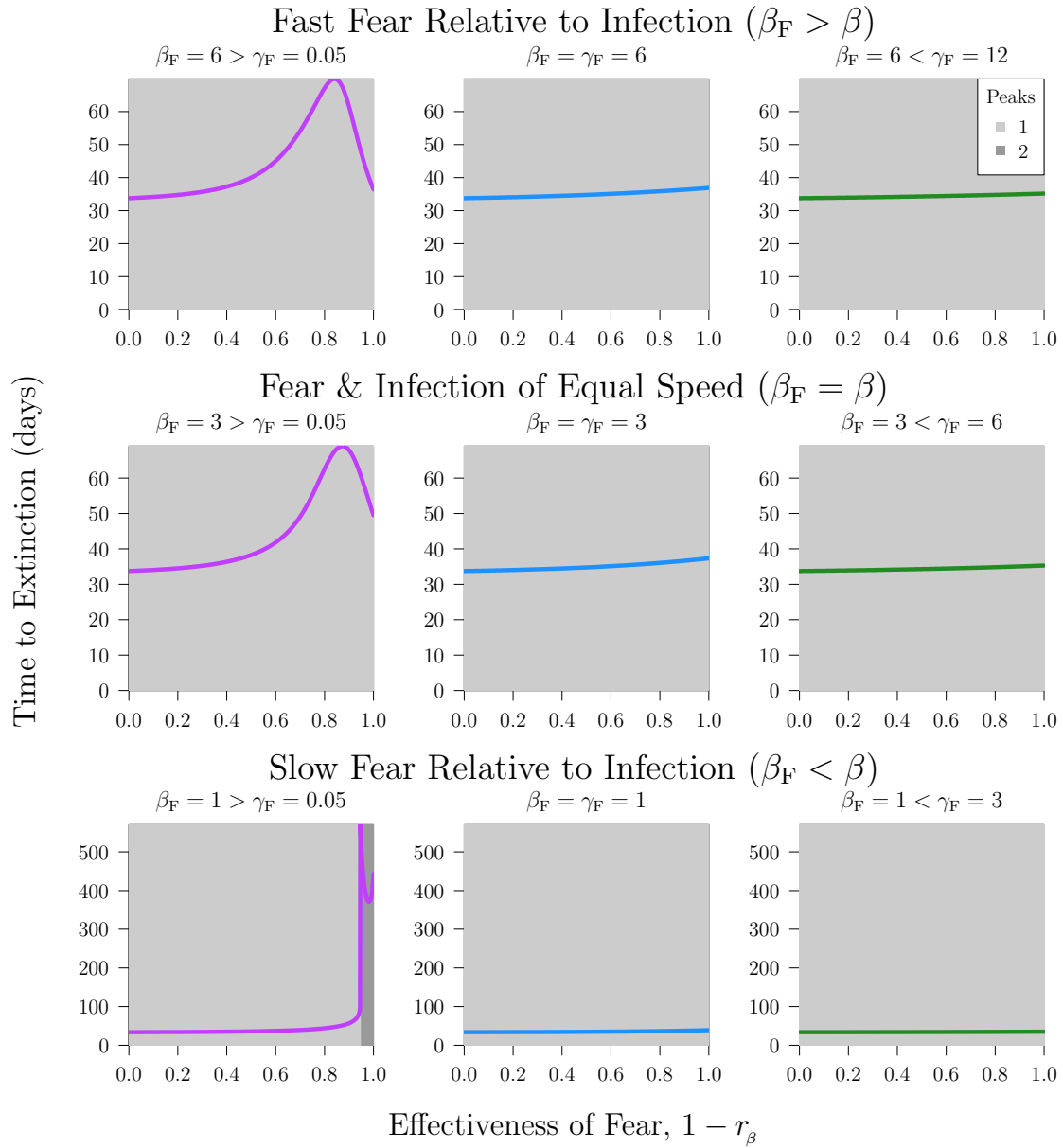


Figure D.4: Outbreak length (time to extinction) as a function of the effectiveness of fear ($1 - r_\beta$) for nine different parameter sets in the bSIR-PF model. Infection parameters and the population size are fixed among the plots, with $\mathcal{R}_0 = 6$, $\gamma = 0.5 \text{ days}^{-1}$ (and thus $\beta = \mathcal{R}_0 \cdot \gamma = 3 \text{ days}^{-1}$), $r_{\beta_F} = 0.2$, and $N = 10^6$ individuals. Fear parameters vary, as given in each plot title.

D.2.2 Final Size

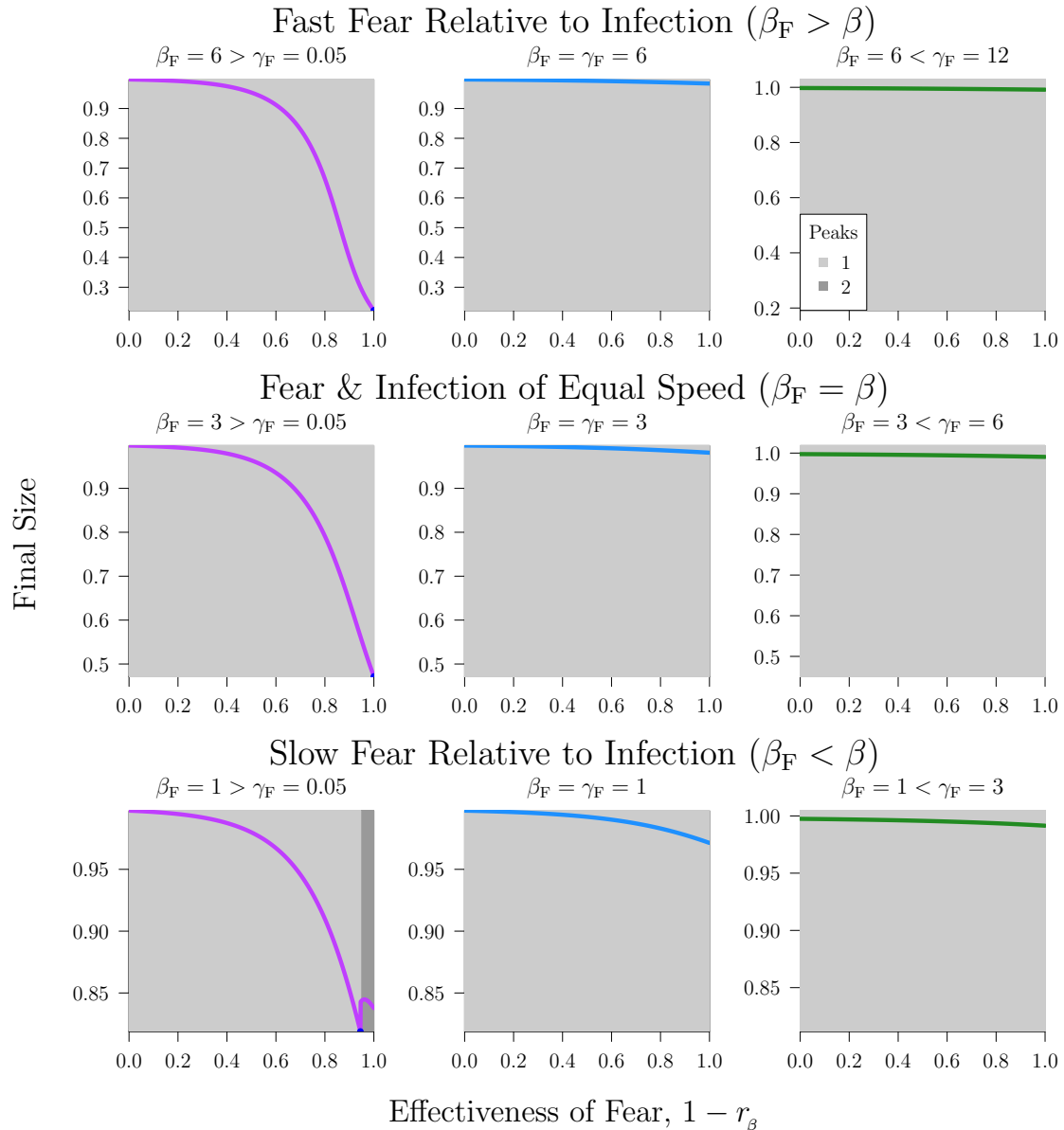


Figure D.5: Final size as a function of the effectiveness of fear ($1 - r_\beta$) for nine different parameter sets in the bSIR-PF model. Parameter values are the same as in figure D.4. The minimum final size is denoted by a blue point.

D.2.3 Peak Prevalences

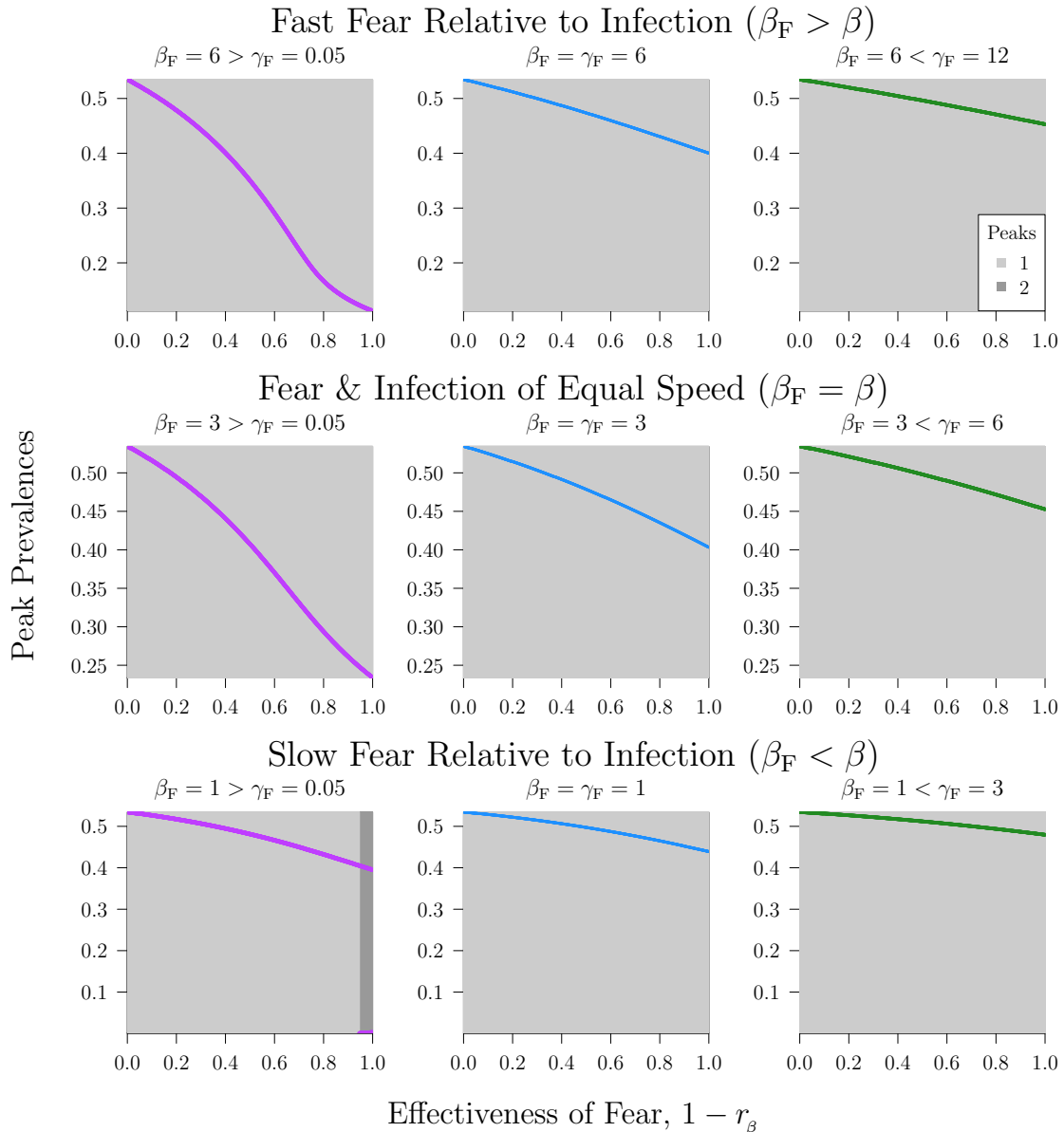


Figure D.6: The peak prevalence of each epidemic as a function of the effectiveness of fear ($1 - r_\beta$) for nine different parameter sets in the bSIR-PF model. Parameter values are the same as in figure 4.5.